Universität Hamburg
DER FORSCHUNG | DER LEHRE | DER BILDUNG

FACULTY
OF MATHEMATICS, INFORMATICS
AND NATURAL SCIENCES



Phenomenology of Direct Dark Matter Detection: DarkSPHERE as a Case Study

24.07.2026

Finn Volker Gallinat
Supervisors: Prof. Dr. Konstantinos Nikolopoulos, Dr. Dimitrios Papoulias

Physics Motivation

- Current DM-experiments using high mass targets (e.g. Xe) lose sensitivity for light DM
- Proposed DarkSPHERE kinematically matched to light DM

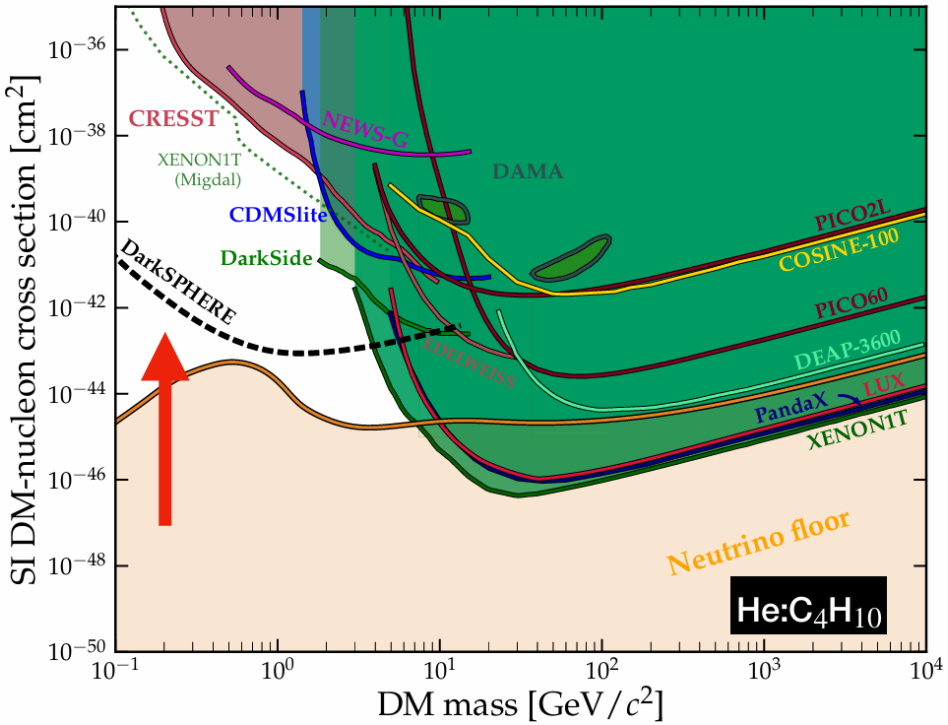

Source: D. Papoulias, HEP 2026 (2026); neutrino fog computed with NeutrinoFog, following C. A. J. O'Hare, Phys. Rev. Lett. 127, 251802 (2021).

How sensitive is DarkSPHERE to light dark matter interactions beyond the standard SI/SD cases?

Recoil rate → NREFT operators → Nuclear responses → Detector model → Sensitivity

Differential Recoil Rate

$$\frac{dR}{dE_R} = \sum_T \frac{\zeta_T}{m_T} \frac{\rho_0}{m_\chi} * \int_{v>v_{min}} v f(\boldsymbol{v} + \boldsymbol{v_E}) \frac{d\sigma_T(v, E_R)}{dE_R} d^3v$$

Detector attributes
- ζ_T: Mass fraction
- m_T: Target mass
- Additional corrections

Astrophysics
- ρ_0: DM density
- m_χ: DM mass
- $f(\boldsymbol{v} + \boldsymbol{v_E})$: Velocity distribution

Dark matter
- $\frac{d\sigma_T(v,E_R)}{dE_R}$: Differential cross section

Nuclear physics
- Nuclear response functions $W_{i,j}^{(N,N')}$

Astrophysical Models

$$\frac{dR}{dE_R} = \sum_T \frac{\zeta_T}{m_T} \frac{\rho_0}{m_\chi} * \int_{v>v_{min}} v f(\boldsymbol{v} + \boldsymbol{v_E}) \frac{d\sigma_T(v, E_R)}{dE_R} d^3v$$

- Standard Halo Model (SHM)
  - Isotropic Maxwellian velocity distribution $f(\boldsymbol{v} + \boldsymbol{v_E})$

Parameter	**Recommended SHM**
Local DM density ρ_0	$0.3\ \mathrm{GeV\,cm^{-3}}$
Circular rotation speed v_0	$238\ \mathrm{km\,s^{-1}}$
Escape speed v_{esc}	$544\ \mathrm{km\,s^{-1}}$

Astrophysical Models

$$\frac{dR}{dE_R} = \sum_T \frac{\zeta_T}{m_T} \frac{\rho_0}{m_\chi} * \int_{v>v_{min}} v f(\boldsymbol{v} + \boldsymbol{v_E}) \frac{d\sigma_T(v, E_R)}{dE_R} d^3v$$

- Standard Halo Model (SHM)
  - Isotropic Maxwellian velocity distribution $f(\boldsymbol{v} + \boldsymbol{v_E})$
- Velocity integrals
  - $g(v_{min}) = \int_{v>v_{min}} \frac{1}{v} f(\boldsymbol{v} + \boldsymbol{v_E}) d^3v \longleftrightarrow \left.\frac{dR}{dE_R}\right|_{\mathrm{SI}} = N_T \frac{m_T A^2 \sigma_{SI} \rho_0}{2\mu^2 m_\chi} F^2(E_R) * \int_{v>v_{min}} \frac{1}{v} f(\boldsymbol{v} + \boldsymbol{v_E}) d^3v$

Astrophysical Models

$$\frac{dR}{dE_R} = \sum_T \frac{\zeta_T}{m_T} \frac{\rho_0}{m_\chi} * \int_{v>v_{min}} v f(\boldsymbol{v} + \boldsymbol{v_E}) \frac{d\sigma_T(v, E_R)}{dE_R} d^3v$$

- Standard Halo Model (SHM)
  - Isotropic Maxwellian velocity distribution $f(\boldsymbol{v} + \boldsymbol{v_E})$
- Velocity integrals
  - $g(v_{min}) = \int_{v>v_{min}} \frac{1}{v} f(\boldsymbol{v} + \boldsymbol{v_E}) d^3v \longleftrightarrow \left.\frac{dR}{dE_R}\right|_{\mathrm{SI}} = N_T \frac{m_T A^2 \sigma_{SI} \rho_0}{2\mu^2 m_\chi} F^2(E_R) * \int_{v>v_{min}} \frac{1}{v} f(\boldsymbol{v} + \boldsymbol{v_E}) d^3v$
  - $h(v_{min}) = \int_{v>v_{min}} v f(\boldsymbol{v} + \boldsymbol{v_E}) d^3v$

Astrophysical Models

$$\frac{dR}{dE_R} = \sum_T \frac{\zeta_T}{m_T} \frac{\rho_0}{m_\chi} * \int_{v>v_{min}} v f(\boldsymbol{v} + \boldsymbol{v_E}) \frac{d\sigma_T(v, E_R)}{dE_R} d^3v$$

- Standard Halo Model (SHM)
  - Isotropic Maxwellian velocity distribution $f(\boldsymbol{v} + \boldsymbol{v_E})$
- Velocity integrals
  - $g(v_{min}) = \int_{v>v_{min}} \frac{1}{v} f(\boldsymbol{v} + \boldsymbol{v_E}) d^3v$
  - $h(v_{min}) = \int_{v>v_{min}} v f(\boldsymbol{v} + \boldsymbol{v_E}) d^3v$

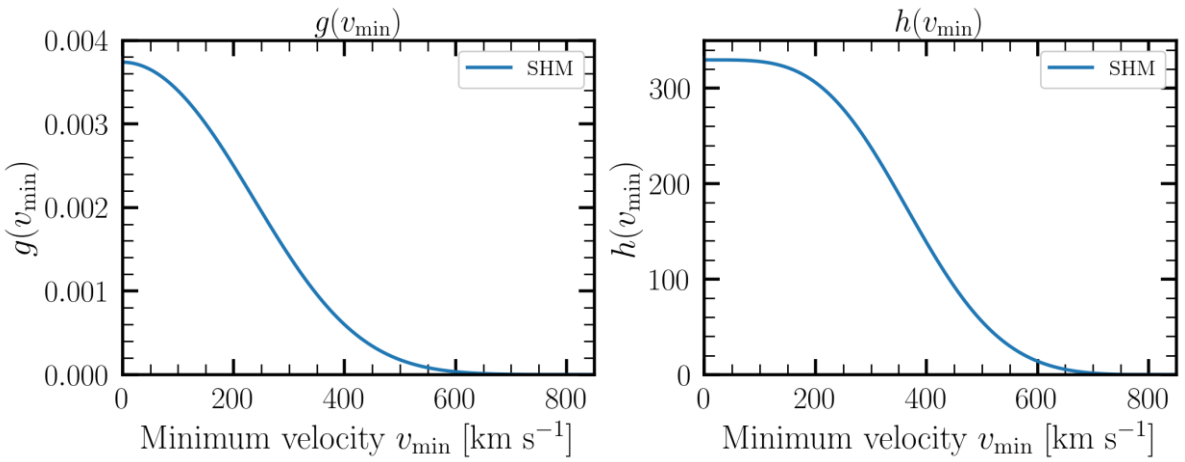

Non-Relativistic Effective Field Theory

$$\frac{dR}{dE_R} = \sum_T \frac{\zeta_T}{m_T}\frac{\rho_0}{m_\chi} * \int_{v>v_{min}} v f(\boldsymbol{v} + \boldsymbol{v_E}) \frac{d\sigma_T(v, E_R)}{dE_R} d^3v$$

- General interaction $\mathcal{L}_{int}(\vec{x}) = c\, \Psi_\chi^*(\vec{x}) \mathcal{O}_\chi \Psi_\chi(\vec{x})\, \Psi_N^*(\vec{x}) \mathcal{O}_N \Psi_N(\vec{x})$

Operators		Hamiltonian		Matrix element	Multipole expansion	Response functions	Square, average over spins	Recoil spectrum
$\mathcal{O}_{NR}^N = \sum_i c_i \mathcal{O}_i^N$	$\boldsymbol{\Sigma_j}$ →	$\widehat{H_T}$	$\langle f\|\widehat{H_T}\|i\rangle$ →	$\mathcal{M}$	→	R_k, W_k	→	$\frac{d\sigma_T(v, E_R)}{dE_R} \propto \lvert\mathcal{M}\rvert^2$

NREFT Operators of DM Interactions

- General NREFT operator
  - $\mathcal{O}_{NR}^{N} = \sum_{\mathrm{i}} c_i \mathcal{O}_{\mathrm{i}}^{N}$
- 4 kinematic quantities:
  - $i\frac{\mathbf{q}}{m_N}$: Momentum transfer
  - $v^{\perp}$: Transverse relative velocity
  - $S_{\chi,N}$: Dark Matter/Nucleon spin
- 14 linear independent operators, linear in velocity on nucleon level

Spin $\frac{1}{2}$

SI

$$\mathcal{O}_1^N \equiv 1,$$

$$\mathcal{O}_3^N \equiv i\,\mathbf{S}_N \cdot \left(\frac{\mathbf{q}}{m_N} \times \mathbf{v}^{\perp}\right),$$

$$\mathcal{O}_5^N \equiv i\,\mathbf{S}_\chi \cdot \left(\frac{\mathbf{q}}{m_N} \times \mathbf{v}^{\perp}\right),$$

$$\mathcal{O}_7^N \equiv \mathbf{S}_N \cdot \mathbf{v}^{\perp},$$

$$\mathcal{O}_9^N \equiv i\,\mathbf{S}_\chi \cdot \left(\mathbf{S}_N \times \frac{\mathbf{q}}{m_N}\right),$$

$$\mathcal{O}_{11}^N \equiv i\,\mathbf{S}_\chi \cdot \frac{\mathbf{q}}{m_N},$$

$$\mathcal{O}_{13}^N \equiv i\left(\mathbf{S}_\chi \cdot \mathbf{v}^{\perp}\right)\left(\mathbf{S}_N \cdot \frac{\mathbf{q}}{m_N}\right),$$

$$\mathcal{O}_{15}^N \equiv \left(\mathbf{S}_\chi \cdot \frac{\mathbf{q}}{m_N}\right)\left[\mathbf{S}_N \cdot \left(\frac{\mathbf{q}}{m_N} \times \mathbf{v}^{\perp}\right)\right],$$

SD

$$\mathcal{O}_4^N \equiv \mathbf{S}_\chi \cdot \mathbf{S}_N,$$

$$\mathcal{O}_6^N \equiv \left(\mathbf{S}_\chi \cdot \frac{\mathbf{q}}{m_N}\right)\left(\mathbf{S}_N \cdot \frac{\mathbf{q}}{m_N}\right),$$

$$\mathcal{O}_8^N \equiv \mathbf{S}_\chi \cdot \mathbf{v}^{\perp},$$

$$\mathcal{O}_{10}^N \equiv i\,\mathbf{S}_N \cdot \frac{\mathbf{q}}{m_N},$$

$$\mathcal{O}_{12}^N \equiv \mathbf{v}^{\perp} \cdot \left(\mathbf{S}_\chi \times \mathbf{S}_N\right),$$

$$\mathcal{O}_{14}^N \equiv i\left(\mathbf{S}_\chi \cdot \frac{\mathbf{q}}{m_N}\right)\left(\mathbf{S}_N \cdot \mathbf{v}^{\perp}\right),$$

Spin 1

$$\mathcal{O}_{16}^N \equiv \left(\mathbf{S}_\chi \cdot \mathbf{v}^{\perp}\right)\left(\mathbf{S}_N \cdot \mathbf{v}^{\perp}\right),$$

$$\mathcal{O}_{17}^N \equiv i\left[\mathbf{S}_\chi \cdot \left(\frac{\mathbf{q}}{m_N} \times \mathbf{v}^{\perp}\right)\right]\left(\mathbf{S}_N \cdot \mathbf{v}^{\perp}\right).$$

DM and Nuclear Responses

- $\overline{|\mathcal{M}|^2} \propto \frac{4\pi}{2J+1} \sum_{k,\tau,\tau'} R_k^{\tau,\tau'} \left(\frac{q^2}{m_N^2}, v_T^{\perp 2} \right) W_k^{\tau,\tau'}(y)$

DM Response $R_k^{\tau,\tau'}$	Nuclear Response $W_k^{\tau,\tau'}$
Determined by operator	Determined by target
Contains kinematic $i\frac{\mathbf{q}}{m_N}$ and $v^{\perp}$ dependence	Contains nuclear form factors and structure
Determines weighting of nuclear channels	Describes nuclear property relevant for scattering

Nuclear Responses

- $\overline{|\mathcal{M}|^2} \propto \frac{4\pi}{2J+1} \sum_{k,\tau,\tau'} R_k^{\tau,\tau'} \left(\frac{q^2}{m_N^2}, v_T^{\perp 2} \right) W_k^{\tau,\tau'}(y)$

Response	Coupling to
M	Charge
Σ', Σ''	Spin density transverse/ longitudinal to $\mathbf{q}$
Δ	Orbital angular momentum
Φ', Φ''	Spin-orbit, spin-velocity

Nuclear Responses

- $\overline{|\mathcal{M}|^2} \propto \frac{4\pi}{2J+1} \sum_{k,\tau,\tau'} R_k^{\tau,\tau'} \left(\frac{q^2}{m_N^2}, v_T^{\perp 2} \right) W_k^{\tau,\tau'}(y)$

Group	Operators	Interpretation
Coherent/charge-like	$\mathcal{O}_1, \mathcal{O}_5, \mathcal{O}_8, \mathcal{O}_{11}$	M-type response; possible q or $v^{\perp}$suppression
Spin-response dominated	$\mathcal{O}_4, \mathcal{O}_6, \mathcal{O}_7, \mathcal{O}_9, \mathcal{O}_{10}$	Σ', Σ''; spin-carrying targets
Mixed/composite response	$\mathcal{O}_3, \mathcal{O}_{12}, \mathcal{O}_{13}, \mathcal{O}_{14}, \mathcal{O}_{15}$	Spin-orbit, velocity, higher-order momenta

Operator groupings

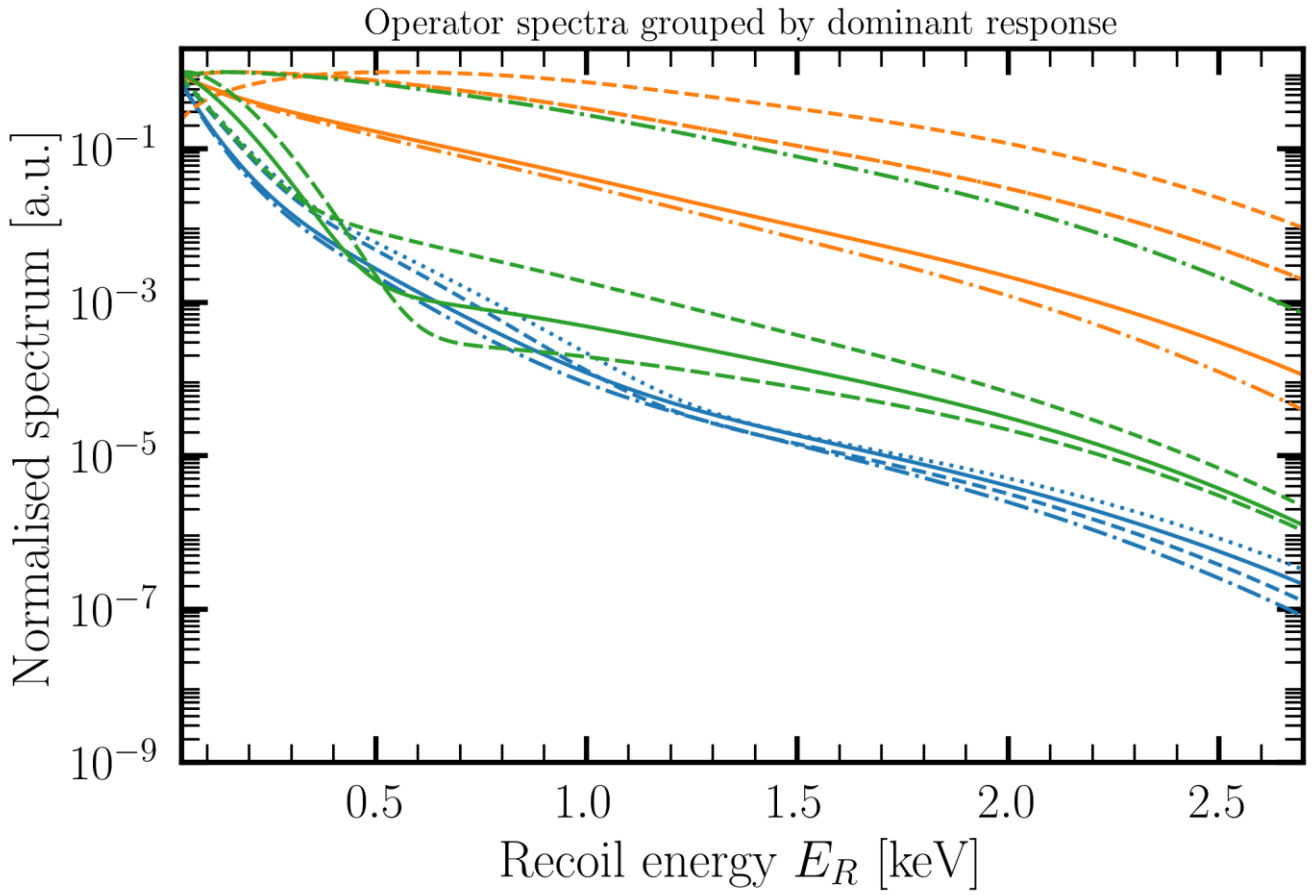

Group	Operators	Colour
Coherent/ charge-like	$\mathcal{O}_1, \mathcal{O}_5, \mathcal{O}_8, \mathcal{O}_{11}$	Blue
Spin-response dominated	$\mathcal{O}_4, \mathcal{O}_6, \mathcal{O}_7, \mathcal{O}_9, \mathcal{O}_{10}$	Orange
Mixed/ composite response	$\mathcal{O}_3, \mathcal{O}_{12}, \mathcal{O}_{13}, \mathcal{O}_{14}, \mathcal{O}_{15}$	Green

DarkSPHERE Detector

- Spherical proportional counter in Boulby underground laboratory
  - He:i-C_4H_{10} gas mixture (90:10)
  - 5 bar pressure, 27.3 kg
  - 300 day exposure, 0.01 dru flat background
  - 14 eV threshold

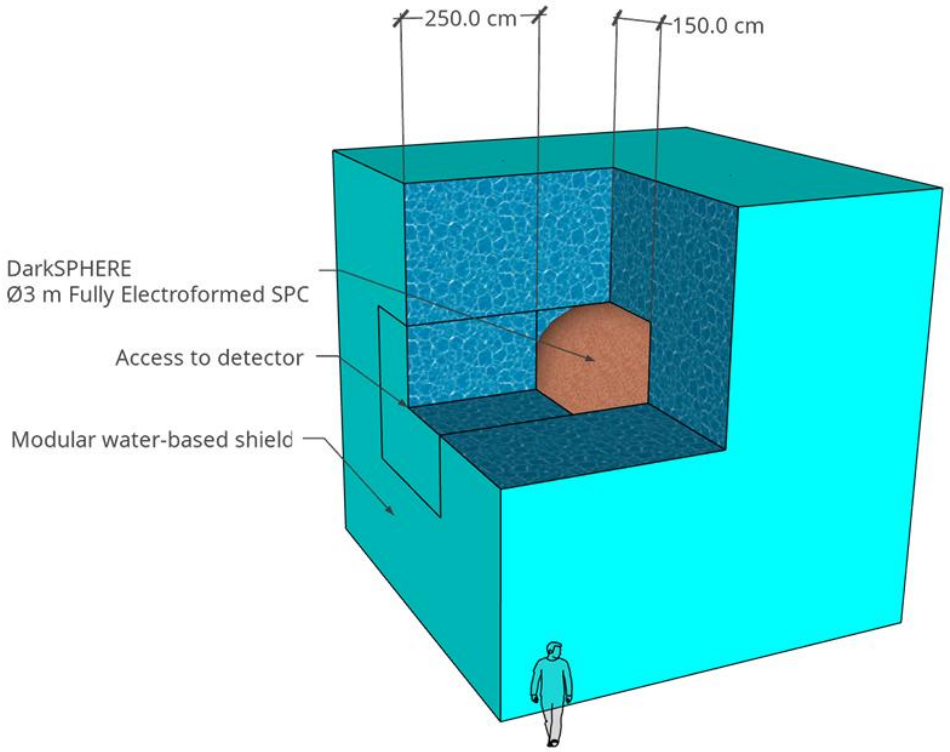

Source: Balogh et al., Phys. Rev. D 108, 112006 (2023), Fig. 9.

Targets suited for light DM detection with complementary responses

Detector Simulation

$$E_{R,true} \rightarrow E_v(E_R) \rightarrow \mathcal{E}_{det} \rightarrow P(\,k \mid E_R\,)$$

- Quenching: $E_v = \mathrm{Q} * E_R$
- Efficiency: $\mathcal{E}_{det}(E, E_{th}, \sigma_{th}) = \frac{1}{2}\left[1 + \mathrm{erf}\left(\frac{E - E_{th}}{\sqrt{2}\sigma_{th}}\right)\right]$
- Resolution and smearing:
  - $E_R \rightarrow P(\,n \mid E_R\,) \rightarrow f(\,E_R \mid n\,) \rightarrow P(\,k \mid E_R\,)$

Detector Simulation - Resolution and Smearing

$$E_{R,true} \rightarrow P(n \mid E_R) \rightarrow f(E_R \mid n) \rightarrow P(k \mid E_R)$$

- $P(n \mid E_R)$: Primary electrons produced
  - COM-Poisson
- $f(E_R \mid n)$: Fluctuation of avalanche gain
  - Number of electrons produces different measured energies
  - Polya distribution
- $P(k \mid E_R)$: Probability for k'th bin with efficiency
  - Integrated over bin

Detector Simulation

$$E_{R,true} \rightarrow E_v(E_R) \rightarrow \mathcal{E}_{det} \rightarrow P(k \mid E_R) \rightarrow s_k$$

- Quenching: $E_v = \mathrm{Q} * E_R$
- Efficiency: $\mathcal{E}_{det}(E, E_{th}, \sigma_{th}) = \frac{1}{2}\left[1 + \mathrm{erf}\left(\frac{E - E_{th}}{\sqrt{2}\sigma_{th}}\right)\right]$
- Resolution and smearing:
  - $E_R \rightarrow P(n \mid E_R) \rightarrow f(E_R \mid n) \rightarrow P(k \mid E_R)$
- Total binned rate:
  - $s_k = t_{\mathrm{exp}} M_{\mathrm{det}} \sum_T \zeta_T \int dE_R \frac{dR_T}{dE_R} P_T(k \mid E_R)$

Exposure = 0.024 ton a

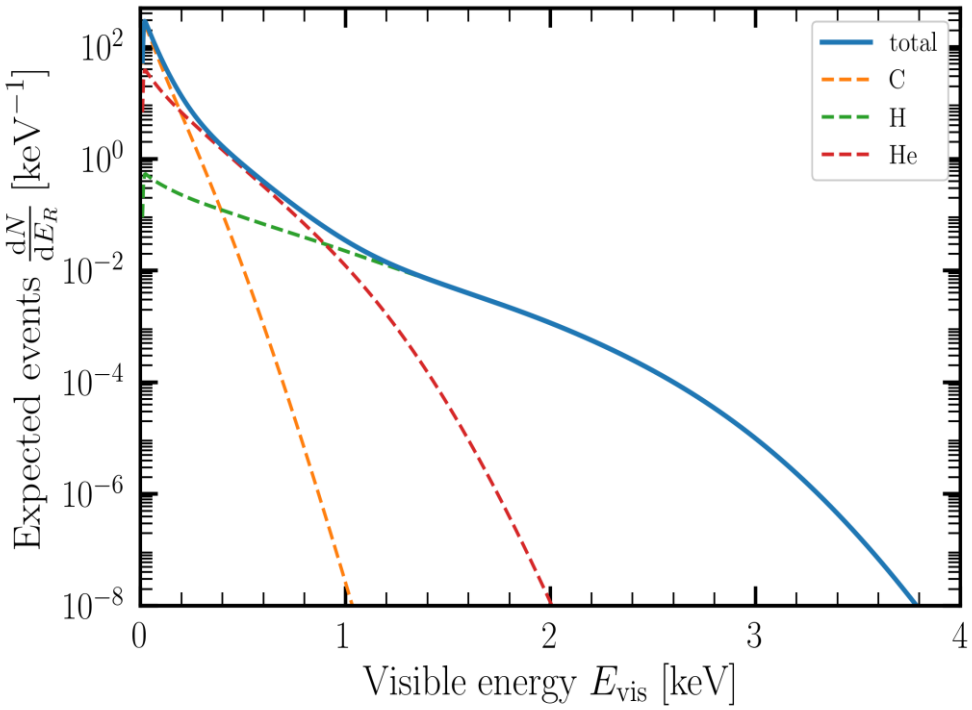

Validation with SI/SD Sensitivities

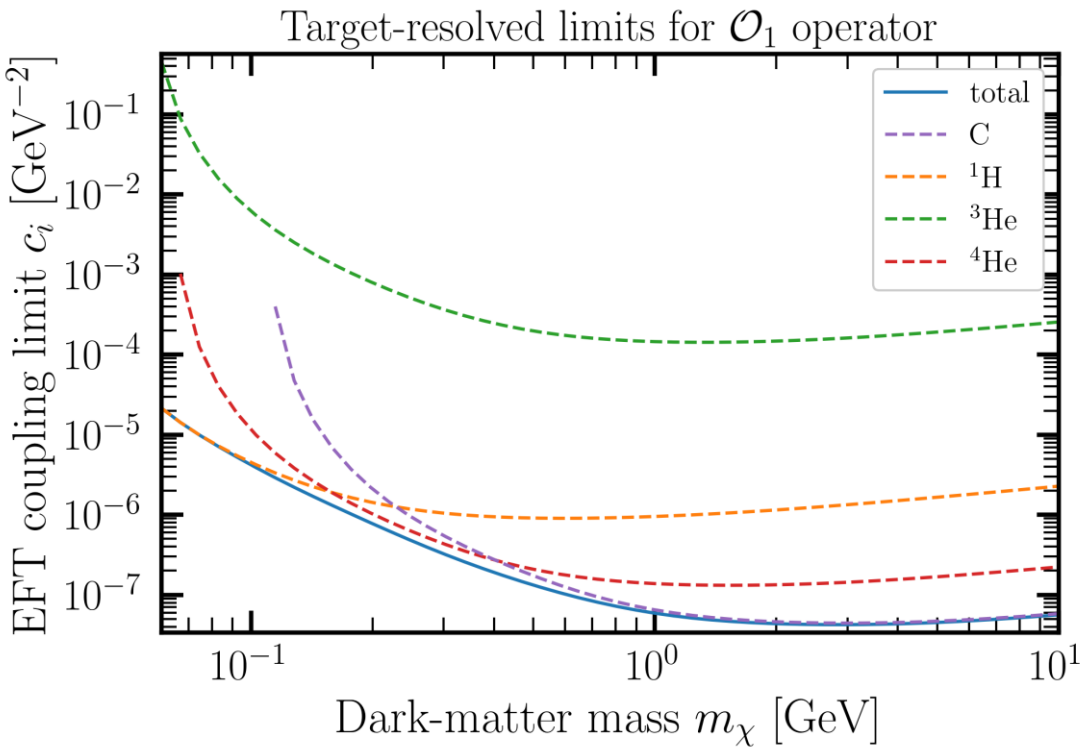

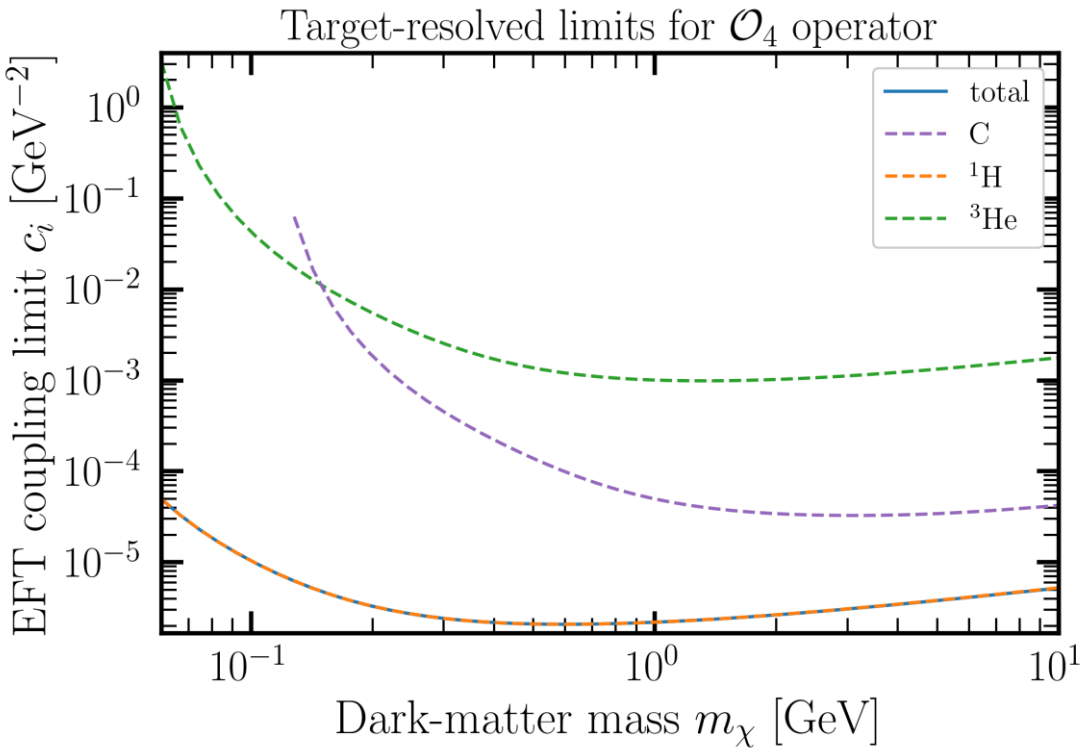

SI/SD Sensitivities in Comparison

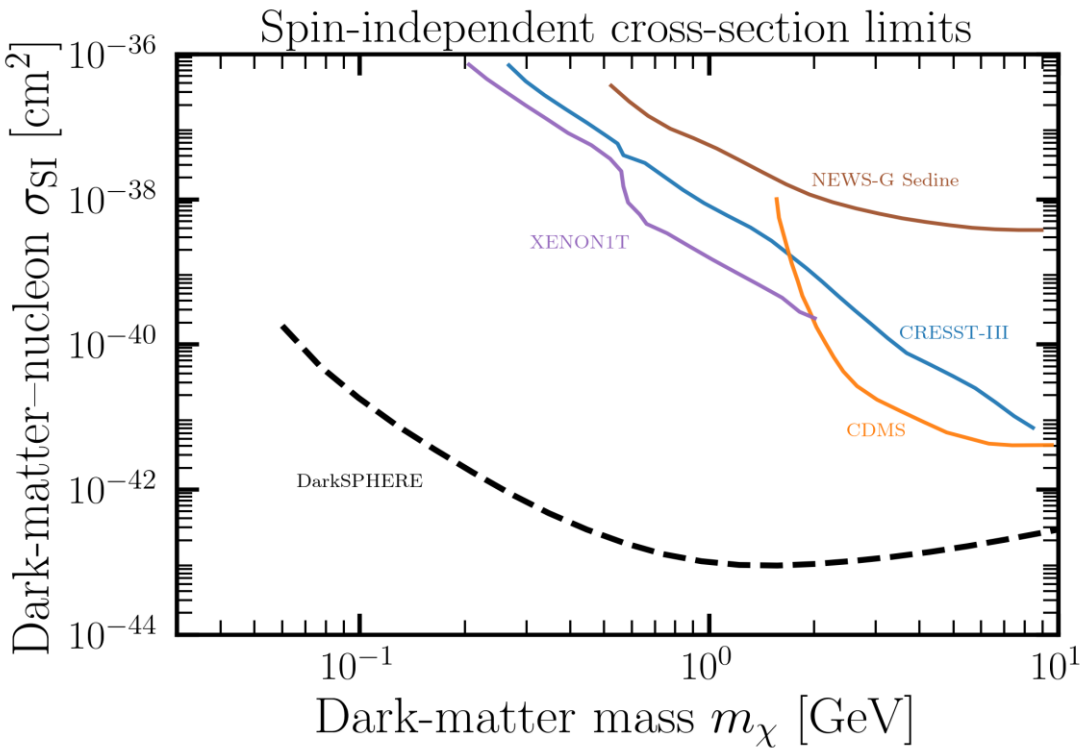

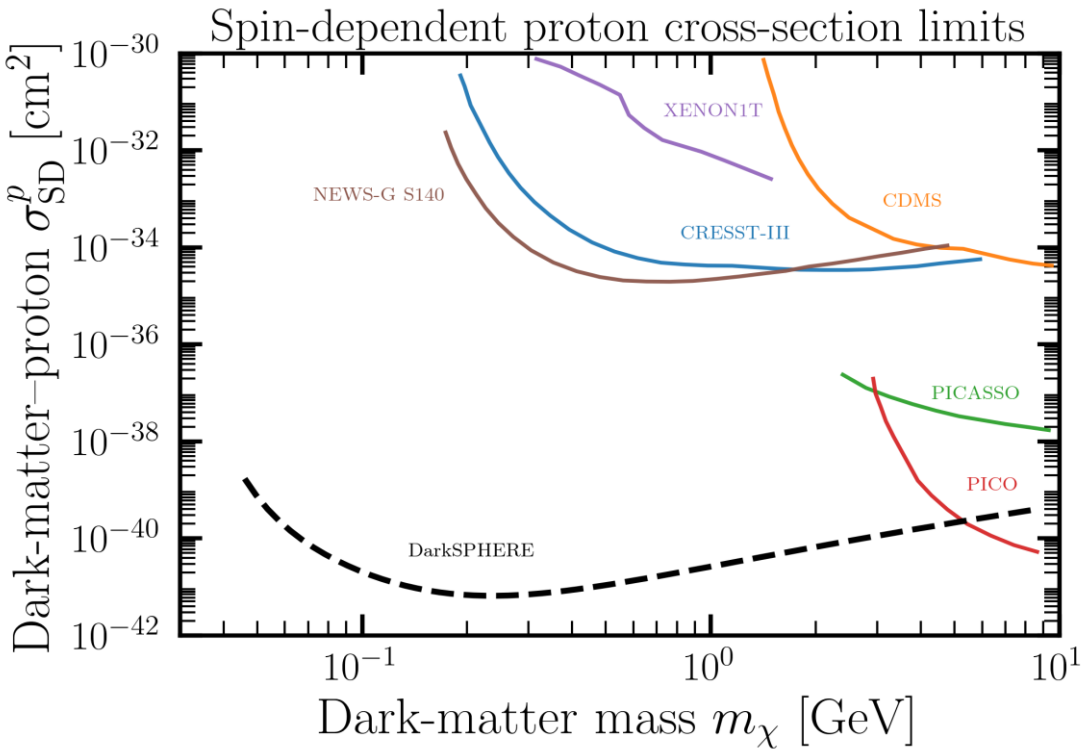

$$\sigma_{SI} = (\hbar c)^2 \frac{\mu^2}{\pi} (c_1)^2$$

$$\sigma_{SD} = \frac{3}{16} (\hbar c)^2 \frac{\mu^2}{\pi} (c_4)^2$$

DarkSPHERE Potential Beyond Standard Interactions

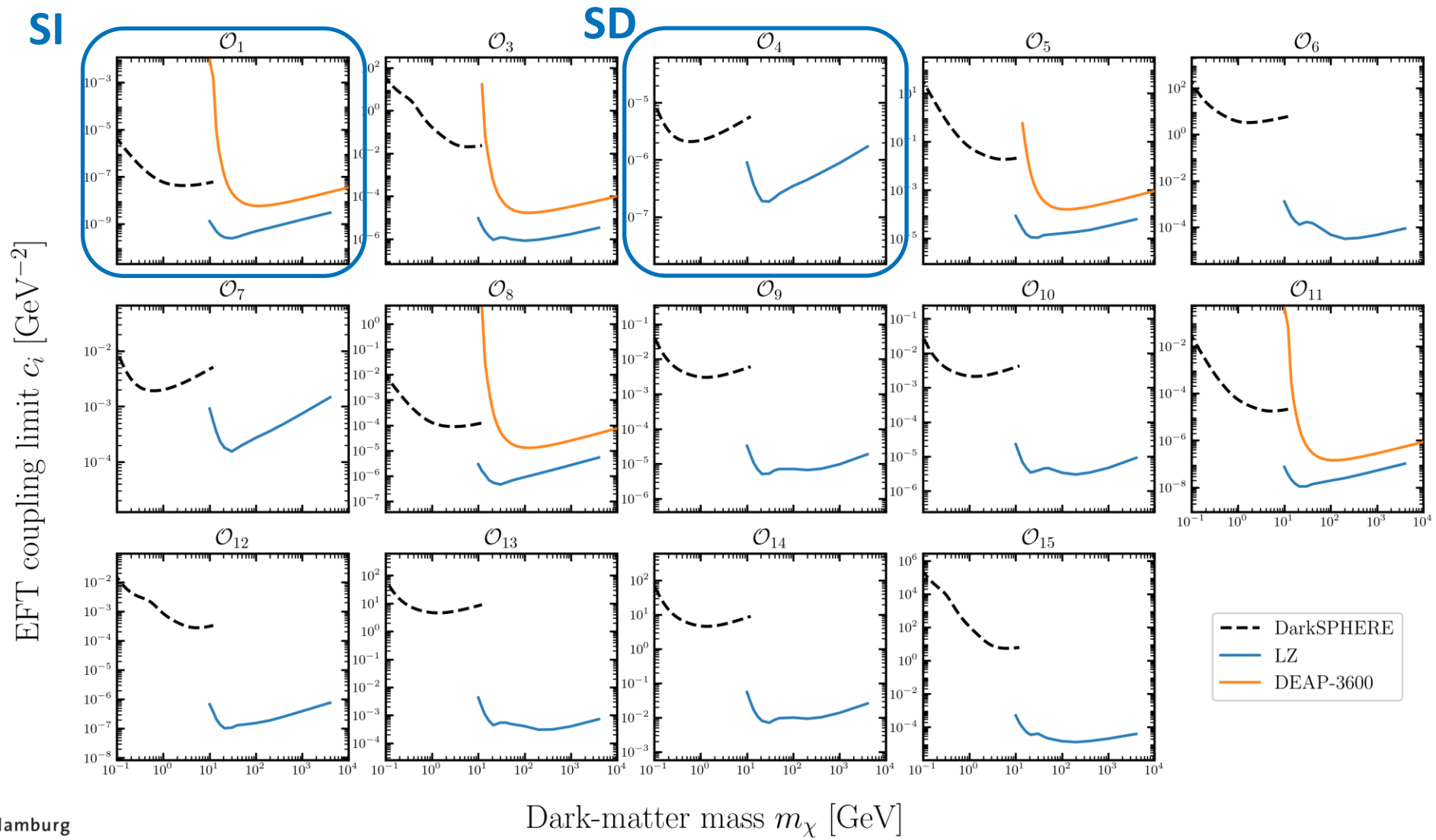

Conclusion and Outlook

- Established framework for direct detection
- Extended analysis beyond standard interactions
- DarkSPHERE reaches new regimes of the light DM parameter space
- Potential of probing interaction beyond SI/SD due to gas composition

- Multi-operator analysis
- Updated detector simulations
- Methods for data analysis, e.g. ML

Thank You For Your Attention

Backup Slides

Backup Slides –Introduction and Framework

Kinematics

- Elastic nuclear recoil induced by DM
  - $E_R^{max} = \frac{2\mu_T^2 v^2}{m_T}$
  - $v_{min}(E_R) = \sqrt{\frac{m_T E_R}{2\mu_T^2}}$
  - $\mu = \frac{m_\chi m_T}{m_\chi + m_T}$

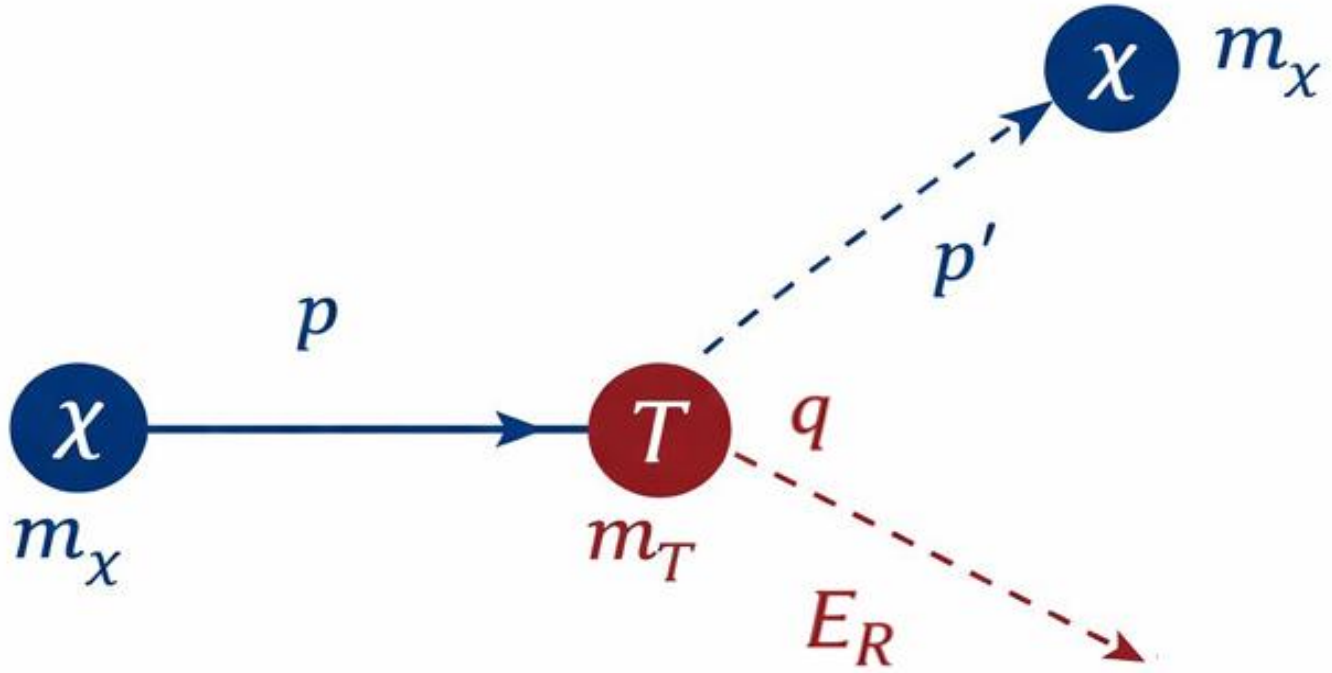

Energy transfer maximised for compatible dark-matter and target masses

SHM++ - Refining the Galactic Halo with Gaia Data

- DM Halo not isotropic due to merger (Evans et al., 2019)
  - $f(\vec{v}) = (1 - \eta) f_R(\vec{v}) + \eta f_S(\vec{v})$;
- $f_S(\vec{v}) = \frac{1}{(2\,\pi)^{3/2}\sigma_R\sigma_\theta^2 N_{S,esc}} \exp(-\frac{v_r^2}{2\sigma_r^2} - \frac{v_\theta^2}{2\sigma_\theta^2} - \frac{v_\phi^2}{2\sigma_\phi^2}) \times \Theta(v_{esc} - |\vec{v}|)$

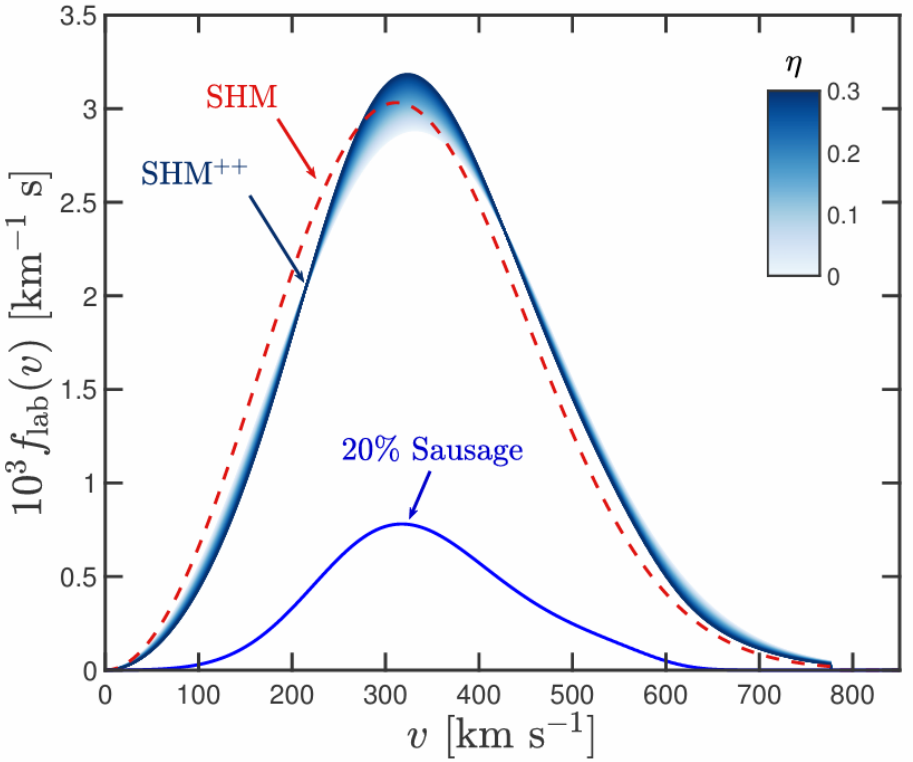

Source: Evans et al., Phys. Rev. D 99, 023012 (2019), Fig. 1.

SHM++ - Refining the Galactic Halo with Gaia Data

- DM Halo not isotropic due to merger
  - $f(\vec{v}) = (1-\eta)f_R(\vec{v}) + \eta f_S(\vec{v})$;
- $f_S(\vec{v}) = \frac{1}{(2\pi)^{3/2}\sigma_R\sigma_\theta^2 N_{S,esc}} \exp(-\frac{v_r^2}{2\sigma_r^2} - \frac{v_\theta^2}{2\sigma_\theta^2} - \frac{v_\phi^2}{2\sigma_\phi^2}) \times \Theta(v_{esc} - |\vec{v}|)$
- Corrected parameters

SHM	Local DM density	ρ_0	$0.3\,\mathrm{GeV\,cm^{-3}}$
	Circular rotation speed	v_0	$220\ \mathrm{km\ s^{-1}}$
	Escape speed	v_{esc}	$544\ \mathrm{km\ s^{-1}}$
	Velocity distribution	$f_{\mathrm{R}}(\mathbf{v})$	Eq. (1)
SHM^{++}	Local DM density	ρ_0	$0.55 \pm 0.17\ \mathrm{GeV\ cm^{-3}}$
	Circular rotation speed	v_0	$233 \pm 3\ \mathrm{km\ s^{-1}}$
	Escape speed	v_{esc}	$528^{+24}_{-25}\ \mathrm{km\ s^{-1}}$
	Sausage anisotropy	β	0.9 ± 0.05
	Sausage fraction	η	0.2 ± 0.1
	Velocity distribution	$f(\mathbf{v})$	Eq. (3)

Source: Evans et al., Phys. Rev. D 99, 023012 (2019), Table I.

SHM++ - Refining the Galactic Halo with Gaia Data

$$\frac{dR}{dE_R} = N_T \frac{\rho_0}{m_D} * \int_{v>v_{min}} v f(\vec{v} + \overrightarrow{v_E}) \frac{d\sigma_T(v, E_R)}{dE_R} d^3v$$

- SI-DM interactions:

$$\frac{dR}{dE_R} = N_T \frac{m_n A^2 \sigma_p \rho_0}{2\mu_p^2 m_D} F^2(E_R) * \int_{v>v_{min}} \frac{1}{v} f(\vec{v} + \overrightarrow{v_E}) d^3v$$

- Velocity dependencies in

$$g(v_{min}) = \int_{v>v_{min}} \frac{1}{v} f(\vec{v} + \overrightarrow{v_E}) d^3v$$

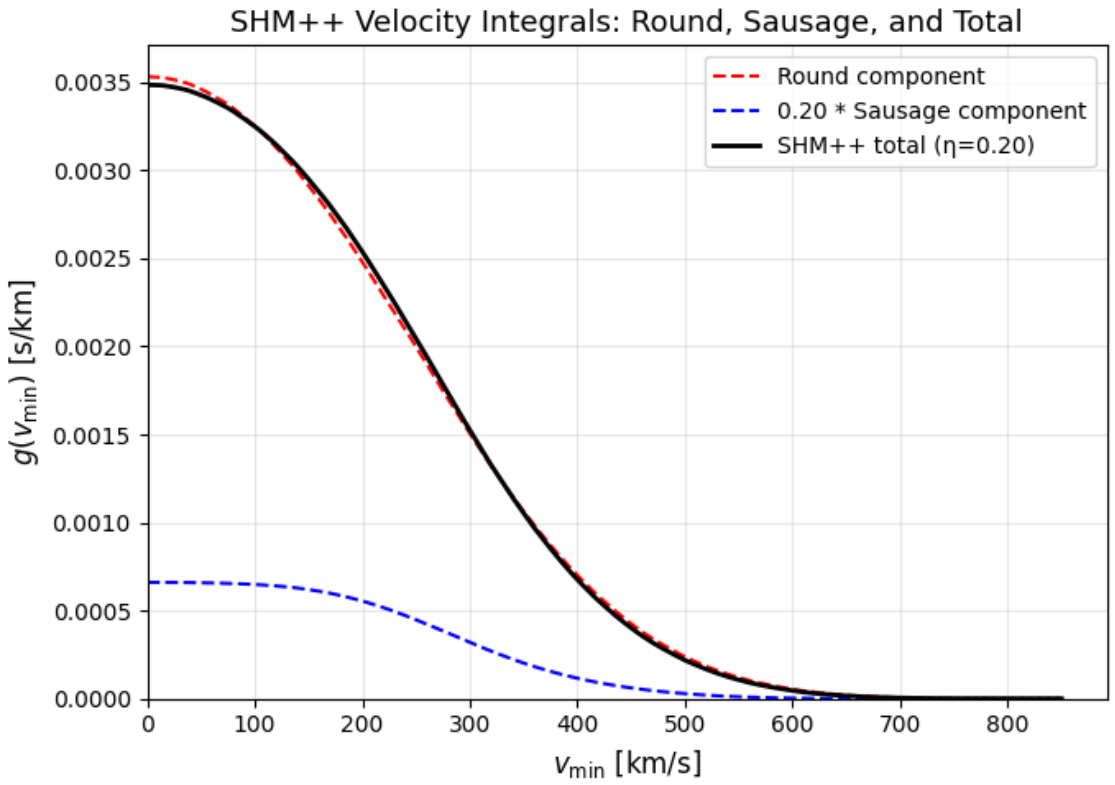

Backup Slides – NREFT

Coupling Convention

$$c_i^{(0)} = c_i^{(n)} + c_i^{(p)}, \qquad c_i^{(1)} = c_i^{(p)} - c_i^{(n)}. \tag{3.9}$$

The general operator in this basis then reads as follows, where we additionally allow non-trivial isospin dependencies in the couplings.

$$\mathcal{O}_{NR}^N = \sum_i (c_i^0 \mathbb{1} + c_i^1 \tau_3)\mathcal{O}_i^N = \sum_{\tau=0,1} \sum_i c_i^\tau \mathcal{O}_i t^\tau, \tag{3.10}$$

The isospin operators are defined as

$$t^0 \equiv \mathbb{1}, \qquad t^1 \equiv \tau_3. \tag{3.11}$$

Dark Matter Physics – NREFT Cross Section

$$\frac{dR}{dE_R} = N_T \frac{\rho_0}{m_\chi} * \int_{v>v_{min}} v f(\vec{v} + \overrightarrow{v_E}) \frac{d\sigma_T(v, E_R)}{dE_R} d^3v$$

- $|\mathcal{M}|^2 \propto \sum_{i,j} \sum_{N,N'=n,p} c_i^N c_j^{N'} F_{i,j}^{(N,N')}(q^2, v_T^{\perp 2})$

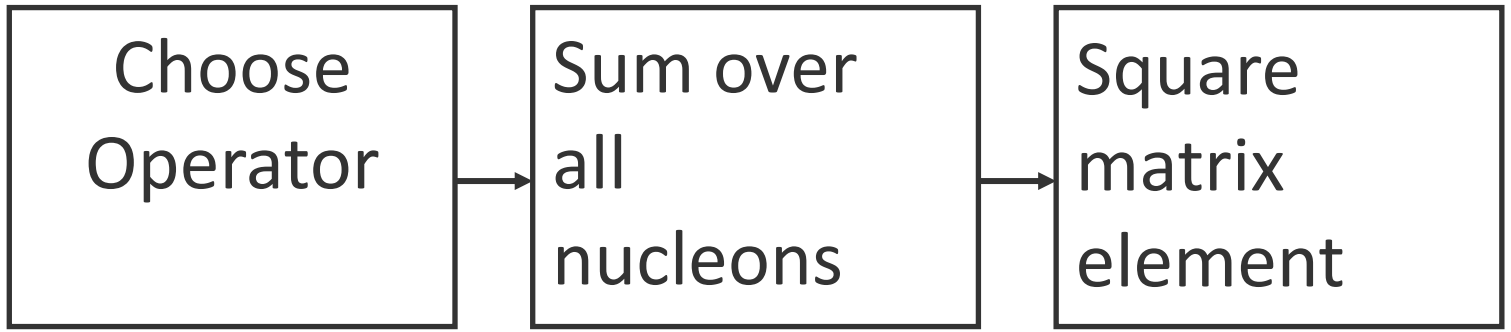

Multipole Expansion

$$\begin{aligned}\mathcal{L}_{\text{EFT}} &= l_0\,1 + l_0^A\left[-2\boldsymbol{v}_N^{\perp}\cdot\boldsymbol{S}_N\right] + \boldsymbol{l}_5\cdot\left[2\boldsymbol{S}_N\right] + \boldsymbol{l}_M\cdot\left[-\boldsymbol{v}_N^{\perp}\right] + \boldsymbol{l}_E\cdot\left[2i\,\boldsymbol{v}_N^{\perp}\times\boldsymbol{S}_N\right] \\ &= l_0\,1 + l_0^A\left(\frac{\boldsymbol{p}_i+\boldsymbol{p}_f}{2m_N}\right)\cdot\boldsymbol{\sigma} + \boldsymbol{l}_5\cdot\boldsymbol{\sigma} + \boldsymbol{l}_M\cdot\left(\frac{\boldsymbol{p}_i+\boldsymbol{p}_f}{2m_N}\right) + \boldsymbol{l}_E\cdot\left(-i\,\frac{\boldsymbol{p}_i+\boldsymbol{p}_f}{2m_N}\times\boldsymbol{\sigma}\right).\end{aligned} \tag{3.15}$$

In order to move to the nuclear description, we first need to calculate the corresponding Hamiltonian density by summing over all nucleons

$$\hat{\mathcal{H}}_T(\boldsymbol{p}) = \sum_{i=1}^{A} l_0\,1 + l_0^A\left(\frac{\boldsymbol{p}_i+\boldsymbol{p}_f}{2m_N}\right)\cdot\boldsymbol{\sigma} + \boldsymbol{l}_5\cdot\boldsymbol{\sigma} + \boldsymbol{l}_M\cdot\left(\frac{\boldsymbol{p}_i+\boldsymbol{p}_f}{2m_N}\right) + \boldsymbol{l}_E\cdot\left(-i\,\frac{\boldsymbol{p}_i+\boldsymbol{p}_f}{2m_N}\times\boldsymbol{\sigma}\right). \tag{3.16}$$

Multipole Expansion

$$\hat{H}_T = \sum_{\tau=0}^{1}\Bigg[\sum_{i=1}^{A} l_0^{\tau}(i)\, e^{-i\boldsymbol{q}\cdot\boldsymbol{x}_i} + \sum_{i=1}^{A} l_0^{A\tau}(i)\,\frac{1}{2m_N}\left[-\frac{1}{i}\overleftarrow{\nabla}_i\cdot\boldsymbol{\sigma}(i)\, e^{-i\boldsymbol{q}\cdot\boldsymbol{x}_i} + e^{-i\boldsymbol{q}\cdot\boldsymbol{x}_i}\,\boldsymbol{\sigma}(i)\cdot\frac{1}{i}\overrightarrow{\nabla}_i\right]$$
$$+ \sum_{i=1}^{A} \boldsymbol{l}_5^{\tau}(i)\cdot\boldsymbol{\sigma}(i)\, e^{-i\boldsymbol{q}\cdot\boldsymbol{x}_i} + \sum_{i=1}^{A} \boldsymbol{l}_M^{\tau}(i)\cdot\frac{1}{2m_N}\left[-\frac{1}{i}\overleftarrow{\nabla}_i\, e^{-i\boldsymbol{q}\cdot\boldsymbol{x}_i} + e^{-i\boldsymbol{q}\cdot\boldsymbol{x}_i}\,\frac{1}{i}\overrightarrow{\nabla}_i\right]$$
$$+ \sum_{i=1}^{A} \boldsymbol{l}_E^{\tau}(i)\cdot\frac{1}{2m_N}\left[\overleftarrow{\nabla}_i\times\boldsymbol{\sigma}(i)\, e^{-i\boldsymbol{q}\cdot\boldsymbol{x}_i} + e^{-i\boldsymbol{q}\cdot\boldsymbol{x}_i}\,\boldsymbol{\sigma}(i)\times\overrightarrow{\nabla}_i\right]\Bigg] t^{\tau}(i).$$

$$e^{i\boldsymbol{q}\cdot\boldsymbol{x}_i} = \sum_{L=0}^{\infty}\sqrt{4\pi}\,[L]\,i^L\, j_L(qx_i)\, Y_{L0}(\Omega_{x_i}),$$

$$\hat{\boldsymbol{e}}_\lambda\, e^{i\boldsymbol{q}\cdot\boldsymbol{x}_i} = \begin{cases} \displaystyle\sum_{L=0}^{\infty}\sqrt{4\pi}\,[L]\,i^{L-1}\frac{\boldsymbol{\nabla}_i}{q}\left[j_L(qx_i)Y_{L0}(\Omega_{x_i})\right], & \lambda = 0, \\ \displaystyle\sum_{L=1}^{\infty}\sqrt{2\pi}\,[L]\,i^{L-2}\left[\lambda j_L(qx_i)\boldsymbol{Y}^{\lambda}_{LL1}(\Omega_{x_i}) + \frac{\boldsymbol{\nabla}_i}{q}\times\left(j_L(qx_i)\boldsymbol{Y}^{\lambda}_{LL1}(\Omega_{x_i})\right)\right], & \lambda = \pm 1. \end{cases}$$

Multipole Expansion

$$
\begin{aligned}
i\mathcal{M}_{fi} &= \langle J, M_J', T, M_T | \, \hat{H}_T(\boldsymbol{q}) \, | J, M_J, T, M_T \rangle \\
&= \sum_{\tau=0}^{1} \sum_{i=1}^{A} \langle J, M_J', T, M_T | \left[\left\langle \hat{l}_0^{\tau}(i) \right\rangle_{\chi} e^{-i\boldsymbol{q}\cdot\boldsymbol{x}_i} \right. \\
&\quad + \left\langle \hat{l}_0^{A\tau}(i) \right\rangle_{\chi} \frac{1}{2m_N} \left(-\frac{1}{i} \overleftarrow{\nabla}_i \cdot \boldsymbol{\sigma}(i) e^{-i\boldsymbol{q}\cdot\boldsymbol{x}_i} + e^{-i\boldsymbol{q}\cdot\boldsymbol{x}_i} \boldsymbol{\sigma}(i) \cdot \frac{1}{i} \overrightarrow{\nabla}_i \right) \\
&\quad + \left\langle \hat{\boldsymbol{l}}_5^{\tau}(i) \right\rangle_{\chi} \cdot \boldsymbol{\sigma}(i) e^{-i\boldsymbol{q}\cdot\boldsymbol{x}_i} \\
&\quad + \left\langle \hat{\boldsymbol{l}}_M^{\tau}(i) \right\rangle_{\chi} \cdot \frac{1}{2m_N} \left(-\frac{1}{i} \overleftarrow{\nabla}_i e^{-i\boldsymbol{q}\cdot\boldsymbol{x}_i} + e^{-i\boldsymbol{q}\cdot\boldsymbol{x}_i} \frac{1}{i} \overrightarrow{\nabla}_i \right) \\
&\quad \left. + \left\langle \hat{\boldsymbol{l}}_E^{\tau}(i) \right\rangle_{\chi} \cdot \frac{1}{2m_N} \left(\overleftarrow{\nabla}_i \times \boldsymbol{\sigma}(i) e^{-i\boldsymbol{q}\cdot\boldsymbol{x}_i} + e^{-i\boldsymbol{q}\cdot\boldsymbol{x}_i} \boldsymbol{\sigma}(i) \times \overrightarrow{\nabla}_i \right) \right] t^{\tau}(i) \, | J, M_J, T, M_T \rangle \, .
\end{aligned}
$$

Multipole Expansion - Example

$$\left\langle \hat{\boldsymbol{l}}_5^\tau \right\rangle_\chi \cdot \sum_{i=1}^{A} \boldsymbol{\sigma}(i) e^{-i\boldsymbol{q}\cdot\boldsymbol{r}_i} t^\tau(i) = \sum_{L=0}^{\infty} \sqrt{4\pi(2L+1)}\,(-i)^L \hat{\Sigma}''_{L0;\tau}(q) \left(\left\langle \hat{\boldsymbol{l}}_5^\tau \right\rangle_\chi \cdot \boldsymbol{e}_0 \right)$$
$$- \sum_{L=1}^{\infty} \sqrt{2\pi(2L+1)}\,(-i)^L \sum_{\lambda=\pm1} \left[\lambda \hat{\Sigma}_{L,-\lambda;\tau}(q) + i\hat{\Sigma}'_{L,-\lambda;\tau}(q) \right]$$
$$\times \left(\left\langle \hat{\boldsymbol{l}}_5^\tau \right\rangle_\chi \cdot \boldsymbol{e}_\lambda \right).$$

Nuclear Responses

- $\overline{|\mathcal{M}|^2} \propto \frac{4\pi}{2J+1} \sum_{k,\tau,\tau'} R_k^{\tau,\tau'} \left(\frac{q^2}{m_N^2}, v_T^{\perp 2} \right) W_k^{\tau,\tau'}(y)$

Response	Coupling to
M	Charge
Σ', Σ''	Spin density transverse/ longitudinal to $\mathbf{q}$
Δ	Orbital angular momentum ℓ
Φ', Φ''	$\boldsymbol{\sigma} \times \boldsymbol{\nabla}$ density $\rightarrow \boldsymbol{\sigma} \cdot \ell$

DM and Nuclear Responses

- $\overline{|\mathcal{M}|^2} \propto \frac{4\pi}{2J+1} \sum_{k,\tau,\tau'} R_k^{\tau,\tau'} \left(\frac{q^2}{m_N^2}, v_T^{\perp 2} \right) W_k^{\tau,\tau'}(y)$

DM response $R_k^{\tau,\tau'}$ × Nuclear Response $W_k^{\tau,\tau'}$

$$
\begin{aligned}
R_M^{\tau\tau'}\left(v_T^{\perp 2}, \frac{q^2}{m_N^2}\right) &= c_1^\tau c_1^{\tau'} + \frac{j_\chi(j_\chi+1)}{3}\left[\frac{q^2}{m_N^2} v_T^{\perp 2} c_5^\tau c_5^{\tau'} + v_T^{\perp 2} c_8^\tau c_8^{\tau'} + \frac{q^2}{m_N^2} c_{11}^\tau c_{11}^{\tau'}\right], \\
R_{\Phi''}^{\tau\tau'}\left(v_T^{\perp 2}, \frac{q^2}{m_N^2}\right) &= \frac{q^2}{4m_N^2} c_3^\tau c_3^{\tau'} + \frac{j_\chi(j_\chi+1)}{12}\left(c_{12}^\tau - \frac{q^2}{m_N^2} c_{15}^\tau\right)\left(c_{12}^{\tau'} - \frac{q^2}{m_N^2} c_{15}^{\tau'}\right), \\
R_{\Phi''M}^{\tau\tau'}\left(v_T^{\perp 2}, \frac{q^2}{m_N^2}\right) &= c_3^\tau c_1^{\tau'} + \frac{j_\chi(j_\chi+1)}{3}\left(c_{12}^\tau - \frac{q^2}{m_N^2} c_{15}^\tau\right) c_{11}^{\tau'}, \\
R_{\Phi'}^{\tau\tau'}\left(v_T^{\perp 2}, \frac{q^2}{m_N^2}\right) &= \frac{j_\chi(j_\chi+1)}{12}\left[c_{12}^\tau c_{12}^{\tau'} + \frac{q^2}{m_N^2} c_{13}^\tau c_{13}^{\tau'}\right], \\
R_{\Sigma''}^{\tau\tau'}\left(v_T^{\perp 2}, \frac{q^2}{m_N^2}\right) &= \frac{q^2}{4m_N^2} c_{10}^\tau c_{10}^{\tau'} + \frac{j_\chi(j_\chi+1)}{12}\left[c_4^\tau c_4^{\tau'} + \frac{q^2}{m_N^2}(c_4^\tau c_6^{\tau'} + c_6^\tau c_4^{\tau'}) + \frac{q^4}{m_N^4} c_6^\tau c_6^{\tau'} + v_T^{\perp 2} c_{12}^\tau c_{12}^{\tau'} + \frac{q^2}{m_N^2} v_T^{\perp 2} c_{13}^\tau c_{13}^{\tau'}\right], \\
R_{\Sigma'}^{\tau\tau'}\left(v_T^{\perp 2}, \frac{q^2}{m_N^2}\right) &= \frac{1}{8}\left[\frac{q^2}{m_N^2} v_T^{\perp 2} c_3^\tau c_3^{\tau'} + v_T^{\perp 2} c_7^\tau c_7^{\tau'}\right] \\
&\quad + \frac{j_\chi(j_\chi+1)}{12}\left[c_4^\tau c_4^{\tau'} + \frac{q^2}{m_N^2} c_9^\tau c_9^{\tau'} + \frac{v_T^{\perp 2}}{2}\left(c_{12}^\tau - \frac{q^2}{m_N^2} c_{15}^\tau\right)\left(c_{12}^{\tau'} - \frac{q^2}{m_N^2} c_{15}^{\tau'}\right) + \frac{q^2}{2m_N^2} v_T^{\perp 2} c_{14}^\tau c_{14}^{\tau'}\right], \\
R_\Delta^{\tau\tau'}\left(v_T^{\perp 2}, \frac{q^2}{m_N^2}\right) &= \frac{j_\chi(j_\chi+1)}{3}\left[\frac{q^2}{m_N^2} c_5^\tau c_5^{\tau'} + c_8^\tau c_8^{\tau'}\right], \\
R_{\Delta\Sigma'}^{\tau\tau'}\left(v_T^{\perp 2}, \frac{q^2}{m_N^2}\right) &= \frac{j_\chi(j_\chi+1)}{3}\left[c_5^\tau c_4^{\tau'} - c_8^\tau c_9^{\tau'}\right].
\end{aligned}
\tag{3.26}
$$

$$
\begin{aligned}
M_{LM}(q\boldsymbol{x}) &\equiv j_L(qx)\, Y_{LM}(\Omega_x), \\
\Sigma'_{LM}(q\boldsymbol{x}) &\equiv -i\left[\frac{1}{q}\boldsymbol{\nabla} \times \boldsymbol{M}_{LL}^M(q\boldsymbol{x})\right] \cdot \boldsymbol{\sigma}, \\
\Sigma''_{LM}(q\boldsymbol{x}) &\equiv \left[\frac{1}{q}\boldsymbol{\nabla} M_{LM}(q\boldsymbol{x})\right] \cdot \boldsymbol{\sigma}, \\
\Delta_{LM}(q\boldsymbol{x}) &\equiv \boldsymbol{M}_{LL}^M(q\boldsymbol{x}) \cdot \frac{1}{q}\boldsymbol{\nabla}, \\
\tilde{\Phi}'_{LM}(q\boldsymbol{x}) &\equiv \left[\left(\frac{1}{q}\boldsymbol{\nabla} \times \boldsymbol{M}_{LL}^M(q\boldsymbol{x})\right) \cdot \left(\boldsymbol{\sigma} \times \frac{1}{q}\boldsymbol{\nabla}\right) + \frac{1}{2}\boldsymbol{M}_{LL}^M(q\boldsymbol{x}) \cdot \boldsymbol{\sigma}\right], \\
\Phi''_{LM}(q\boldsymbol{x}) &\equiv i\left(\frac{1}{q}\boldsymbol{\nabla} M_{LM}(q\boldsymbol{x})\right) \cdot \left(\boldsymbol{\sigma} \times \frac{1}{q}\boldsymbol{\nabla}\right).
\end{aligned}
$$

Nuclear Responses

- $\overline{|\mathcal{M}|^2} \propto \frac{4\pi}{2J+1} \sum_{k,\tau,\tau'} R_k^{\tau,\tau'} \left(\frac{q^2}{m_N^2}, v_T^{\perp 2} \right) W_k^{\tau,\tau'}(y)$

$$M_{LM}(q\boldsymbol{x}) \equiv j_L(qx)\, Y_{LM}(\Omega_x),$$

$$\Sigma'_{LM}(q\boldsymbol{x}) \equiv -i \left[\frac{1}{q} \boldsymbol{\nabla} \times \boldsymbol{M}^M_{LL}(q\boldsymbol{x}) \right] \cdot \boldsymbol{\sigma},$$

$$\Sigma''_{LM}(q\boldsymbol{x}) \equiv \left[\frac{1}{q} \boldsymbol{\nabla} M_{LM}(q\boldsymbol{x}) \right] \cdot \boldsymbol{\sigma},$$

$$\Delta_{LM}(q\boldsymbol{x}) \equiv \boldsymbol{M}^M_{LL}(q\boldsymbol{x}) \cdot \frac{1}{q} \boldsymbol{\nabla},$$

$$\tilde{\Phi}'_{LM}(q\boldsymbol{x}) \equiv \left[\left(\frac{1}{q} \boldsymbol{\nabla} \times \boldsymbol{M}^M_{LL}(q\boldsymbol{x}) \right) \cdot \left(\boldsymbol{\sigma} \times \frac{1}{q} \boldsymbol{\nabla} \right) + \frac{1}{2} \boldsymbol{M}^M_{LL}(q\boldsymbol{x}) \cdot \boldsymbol{\sigma} \right],$$

$$\Phi''_{LM}(q\boldsymbol{x}) \equiv i \left(\frac{1}{q} \boldsymbol{\nabla} M_{LM}(q\boldsymbol{x}) \right) \cdot \left(\boldsymbol{\sigma} \times \frac{1}{q} \boldsymbol{\nabla} \right).$$

Nuclear Responses

- $\overline{|\mathcal{M}|^2} \propto \frac{4\pi}{2J+1} \sum_{k,\tau,\tau'} R_k^{\tau,\tau'} \left(\frac{q^2}{m_N^2}, v_T^{\perp 2} \right) W_k^{\tau,\tau'}(y)$

H

$$W_M^{00}(y) = W_M^{11}(y) = W_M^{10}(y) = W_M^{01}(y) = 0.0397887, \quad \text{(C.8)}$$
$$W_{\Sigma''}^{00}(y) = W_{\Sigma''}^{11}(y) = W_{\Sigma''}^{10}(y) = W_{\Sigma''}^{01}(y) = 0.0397887, \quad \text{(C.9)}$$
$$W_{\Sigma'}^{00}(y) = W_{\Sigma'}^{11}(y) = W_{\Sigma'}^{10}(y) = W_{\Sigma'}^{01}(y) = 0.0795775. \quad \text{(C.10)}$$

^{3}He

$$W_M^{00}(y) = 0.358099\, e^{-2y}, \quad \text{(C.11)}$$
$$W_M^{11}(y) = 0.0397887\, e^{-2y}, \quad \text{(C.12)}$$
$$W_M^{10}(y) = W_M^{01}(y) = 0.119366\, e^{-2y}. \quad \text{(C.13)}$$

$$W_{\Sigma''}^{00}(y) = W_{\Sigma''}^{11}(y) = 0.0397887\, e^{-2y}, \quad \text{(C.14)}$$
$$W_{\Sigma''}^{10}(y) = W_{\Sigma''}^{01}(y) = -0.0397887\, e^{-2y}, \quad \text{(C.15)}$$
$$W_{\Sigma'}^{00}(y) = W_{\Sigma'}^{11}(y) = 0.0795775\, e^{-2y}, \quad \text{(C.16)}$$
$$W_{\Sigma'}^{10}(y) = W_{\Sigma'}^{01}(y) = -0.0795775\, e^{-2y}. \quad \text{(C.17)}$$

Nuclear Responses

- $\overline{|\mathcal{M}|^2} \propto \frac{4\pi}{2J+1} \sum_{k,\tau,\tau'} R_k^{\tau,\tau'} \left(\frac{q^2}{m_N^2}, v_T^{\perp 2} \right) W_k^{\tau,\tau'}(y)$

^{4}He

$$W_M^{00}(y) = 0.318310\, e^{-2y}. \tag{C.18}$$

^{12}C

$$W_M^{00}(y) = 0.565882\, e^{-2y}\, (2.25 - y)^2, \tag{C.19}$$

$$W_{\Phi''}^{00}(y) = 0.0480805\, e^{-2y}, \tag{C.20}$$

$$W_{M\Phi''}^{00}(y) = e^{-2y}\, (-0.371134 + 0.164948\, y)\,. \tag{C.21}$$

DM Responses

- $\overline{|\mathcal{M}|^2} \propto \frac{4\pi}{2J+1} \sum_{k,\tau,\tau'} R_k^{\tau,\tau'} \left(\frac{q^2}{m_N^2}, v_T^{\perp 2} \right) W_k^{\tau,\tau'}(y)$

$$
\begin{aligned}
R_M^{\tau\tau'}\left(\boldsymbol{v}_T^{\perp 2}, \frac{\boldsymbol{q}^2}{m_N^2}\right) &= c_1^\tau c_1^{\tau'} + \frac{j_\chi(j_\chi+1)}{3}\left[\frac{\boldsymbol{q}^2}{m_N^2}\boldsymbol{v}_T^{\perp 2} c_5^\tau c_5^{\tau'} + \boldsymbol{v}_T^{\perp 2} c_8^\tau c_8^{\tau'} + \frac{\boldsymbol{q}^2}{m_N^2} c_{11}^\tau c_{11}^{\tau'}\right], \\
R_{\Phi''}^{\tau\tau'}\left(\boldsymbol{v}_T^{\perp 2}, \frac{\boldsymbol{q}^2}{m_N^2}\right) &= \frac{\boldsymbol{q}^2}{4m_N^2} c_3^\tau c_3^{\tau'} + \frac{j_\chi(j_\chi+1)}{12}\left(c_{12}^\tau - \frac{\boldsymbol{q}^2}{m_N^2} c_{15}^\tau\right)\left(c_{12}^{\tau'} - \frac{\boldsymbol{q}^2}{m_N^2} c_{15}^{\tau'}\right), \\
R_{\Phi''M}^{\tau\tau'}\left(\boldsymbol{v}_T^{\perp 2}, \frac{\boldsymbol{q}^2}{m_N^2}\right) &= c_3^\tau c_1^{\tau'} + \frac{j_\chi(j_\chi+1)}{3}\left(c_{12}^\tau - \frac{\boldsymbol{q}^2}{m_N^2} c_{15}^\tau\right) c_{11}^{\tau'}, \\
R_{\Phi'}^{\tau\tau'}\left(\boldsymbol{v}_T^{\perp 2}, \frac{\boldsymbol{q}^2}{m_N^2}\right) &= \frac{j_\chi(j_\chi+1)}{12}\left[c_{12}^\tau c_{12}^{\tau'} + \frac{\boldsymbol{q}^2}{m_N^2} c_{13}^\tau c_{13}^{\tau'}\right], \\
R_{\Sigma''}^{\tau\tau'}\left(\boldsymbol{v}_T^{\perp 2}, \frac{\boldsymbol{q}^2}{m_N^2}\right) &= \frac{\boldsymbol{q}^2}{4m_N^2} c_{10}^\tau c_{10}^{\tau'} + \frac{j_\chi(j_\chi+1)}{12}\left[c_4^\tau c_4^{\tau'} + \frac{\boldsymbol{q}^2}{m_N^2}(c_4^\tau c_6^{\tau'} + c_6^\tau c_4^{\tau'}) + \frac{\boldsymbol{q}^4}{m_N^4} c_6^\tau c_6^{\tau'} + \boldsymbol{v}_T^{\perp 2} c_{12}^\tau c_{12}^{\tau'} + \frac{\boldsymbol{q}^2}{m_N^2}\boldsymbol{v}_T^{\perp 2} c_{13}^\tau c_{13}^{\tau'}\right], \\
R_{\Sigma'}^{\tau\tau'}\left(\boldsymbol{v}_T^{\perp 2}, \frac{\boldsymbol{q}^2}{m_N^2}\right) &= \frac{1}{8}\left[\frac{\boldsymbol{q}^2}{m_N^2}\boldsymbol{v}_T^{\perp 2} c_3^\tau c_3^{\tau'} + \boldsymbol{v}_T^{\perp 2} c_7^\tau c_7^{\tau'}\right] \\
&\quad + \frac{j_\chi(j_\chi+1)}{12}\left[c_4^\tau c_4^{\tau'} + \frac{\boldsymbol{q}^2}{m_N^2} c_9^\tau c_9^{\tau'} + \frac{\boldsymbol{v}_T^{\perp 2}}{2}\left(c_{12}^\tau - \frac{\boldsymbol{q}^2}{m_N^2} c_{15}^\tau\right)\left(c_{12}^{\tau'} - \frac{\boldsymbol{q}^2}{m_N^2} c_{15}^{\tau'}\right) + \frac{\boldsymbol{q}^2}{2m_N^2}\boldsymbol{v}_T^{\perp 2} c_{14}^\tau c_{14}^{\tau'}\right], \\
R_\Delta^{\tau\tau'}\left(\boldsymbol{v}_T^{\perp 2}, \frac{\boldsymbol{q}^2}{m_N^2}\right) &= \frac{j_\chi(j_\chi+1)}{3}\left[\frac{\boldsymbol{q}^2}{m_N^2} c_5^\tau c_5^{\tau'} + c_8^\tau c_8^{\tau'}\right], \\
R_{\Delta\Sigma'}^{\tau\tau'}\left(\boldsymbol{v}_T^{\perp 2}, \frac{\boldsymbol{q}^2}{m_N^2}\right) &= \frac{j_\chi(j_\chi+1)}{3}\left[c_5^\tau c_4^{\tau'} - c_8^\tau c_9^{\tau'}\right].
\end{aligned}
\tag{3.26}
$$

Formfactors

$$F_X^{(N,N')}(q^2) \equiv \frac{4\pi}{2J+1}\sum_L \langle J\|\hat{X}_L^{(N)}(q)\|J\rangle\langle J\|\hat{X}_L^{(N')}(q)\|J\rangle, \tag{3.27}$$

$$F_{X,Y}^{(N,N')}(q^2) \equiv \frac{4\pi}{2J+1}\sum_L \langle J\|\hat{X}_L^{(N)}(q)\|J\rangle\langle J\|\hat{Y}_L^{(N')}(q)\|J\rangle, \tag{3.28}$$

the matrix element can be written as

$$\frac{1}{2j_\chi+1}\frac{1}{2J+1}\sum_{\text{spins}}|\mathcal{M}|^2 = \frac{m_T^2}{m_N^2}\sum_{i,j}\sum_{\tau,\tau'=0,1} c_i^\tau c_j^{\tau'} F_{ij}^{\tau\tau'}\left(\boldsymbol{v}_T^{\perp\,2}, \frac{q^2}{m_N^2}\right). \tag{3.29}$$

In this text we follow the convention of Reference [18] using the classification through the nuclear responses. An overview of those for the used isotopes in this text, adapted from References [16, 18], is provided in Appendix C.2. If one prefers to work with the form factors, those can be easily converted through Equation 3.30

$$F_{AB}^{\tau\tau'}(q^2) = \frac{4\pi}{2J+1}W_{AB}^{\tau\tau'}(y). \tag{3.30}$$

Backup Slides – DarkSPHERE

DarkSPHERE Detector

- Spherical proportional counter in Boulby underground laboratory
  - He:i-C_4H_{10} gas mixture (90:10)
  - 5 bar pressure, 27.3 kg
  - 300 day exposure, 0.01 dru flat background
  - 14 eV threshold

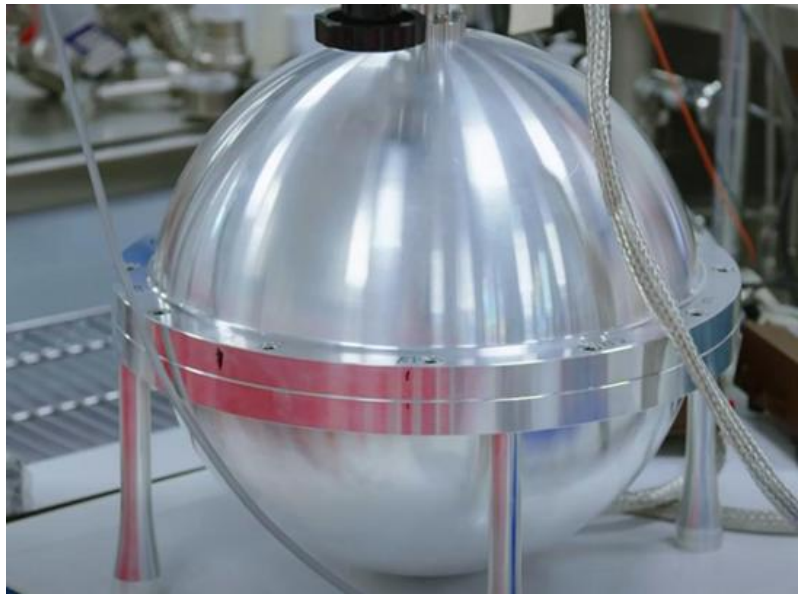

R&D sphere

Targets suited for light DM detection with complementary responses

Maximum Likelihood Analysis

- $\lambda_k(\mu) = \mu s_k + b_k$
  - s_k: Signal per bin; b_k: background
- Assume Asimov dataset ($n_k = b_k, \hat{\mu} = 0$):
  - $L(\mu) = \prod_k Pois(n_k|\mu s_k + b_k)$
  - $q_\mu = -2ln\frac{L(\mu)}{L(\hat{\mu})}$
- Solve for $q_{crit} = 1.64$ (one-sided $\chi^2(1)$)
  - $c_{lim} = c_{ref}\sqrt{\mu_{lim}}$

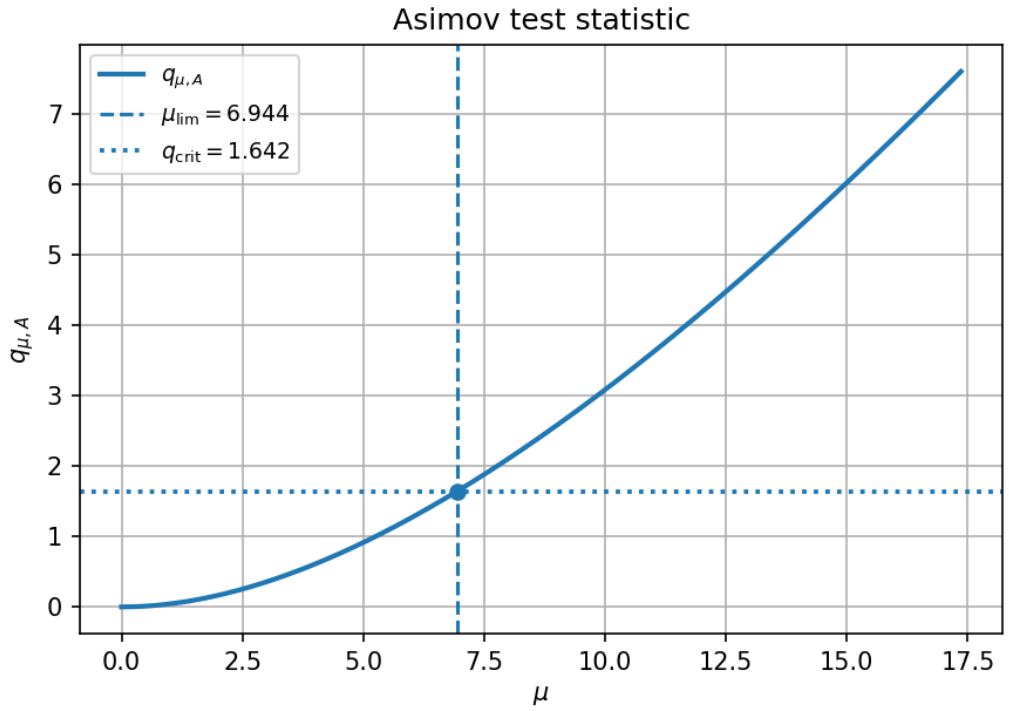

Quenching and Efficiency

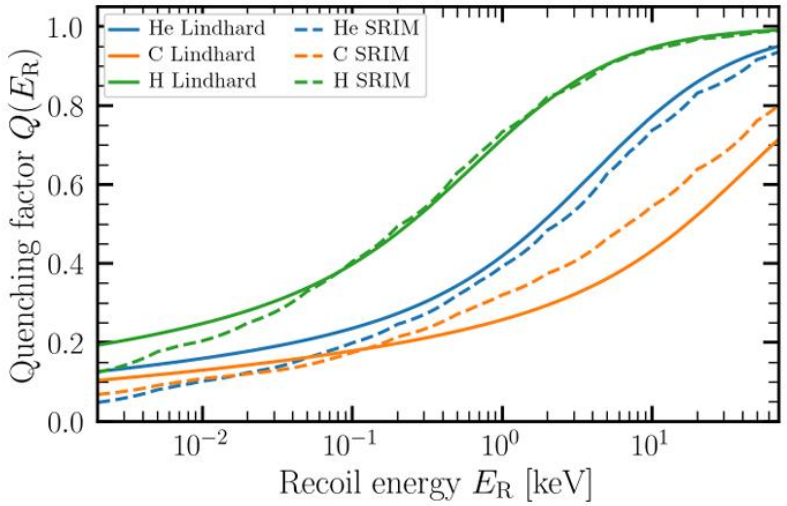

(a) Quenching factors.

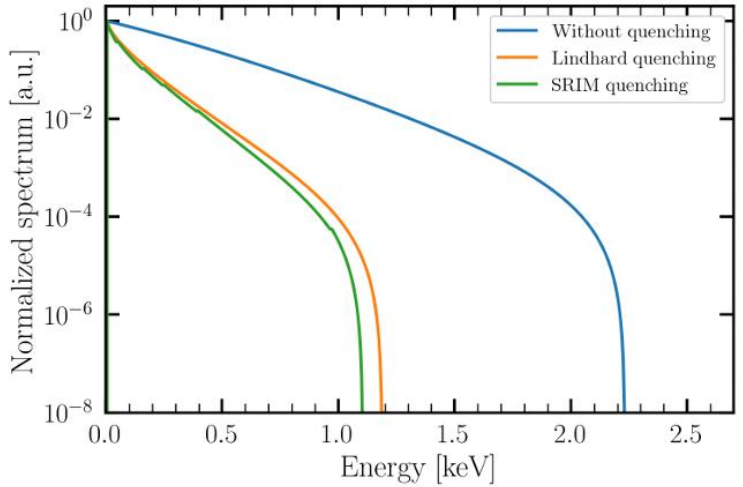

(b) Impact on the spectrum for a helium target.

Lindhard

$$Q = \frac{kg(\epsilon_L)}{1 + kg(\epsilon_L)},$$

$$\epsilon_L = 11.5 E_R(\text{keV}) Z^{-\frac{7}{3}},$$
$$k = 0.133 Z^{\frac{2}{3}} A^{-\frac{1}{2}},$$
$$g(\epsilon_L) = 3\epsilon_L^{0.15} + 0.7\epsilon_L^{0.6} + \epsilon_L.$$

Efficiency

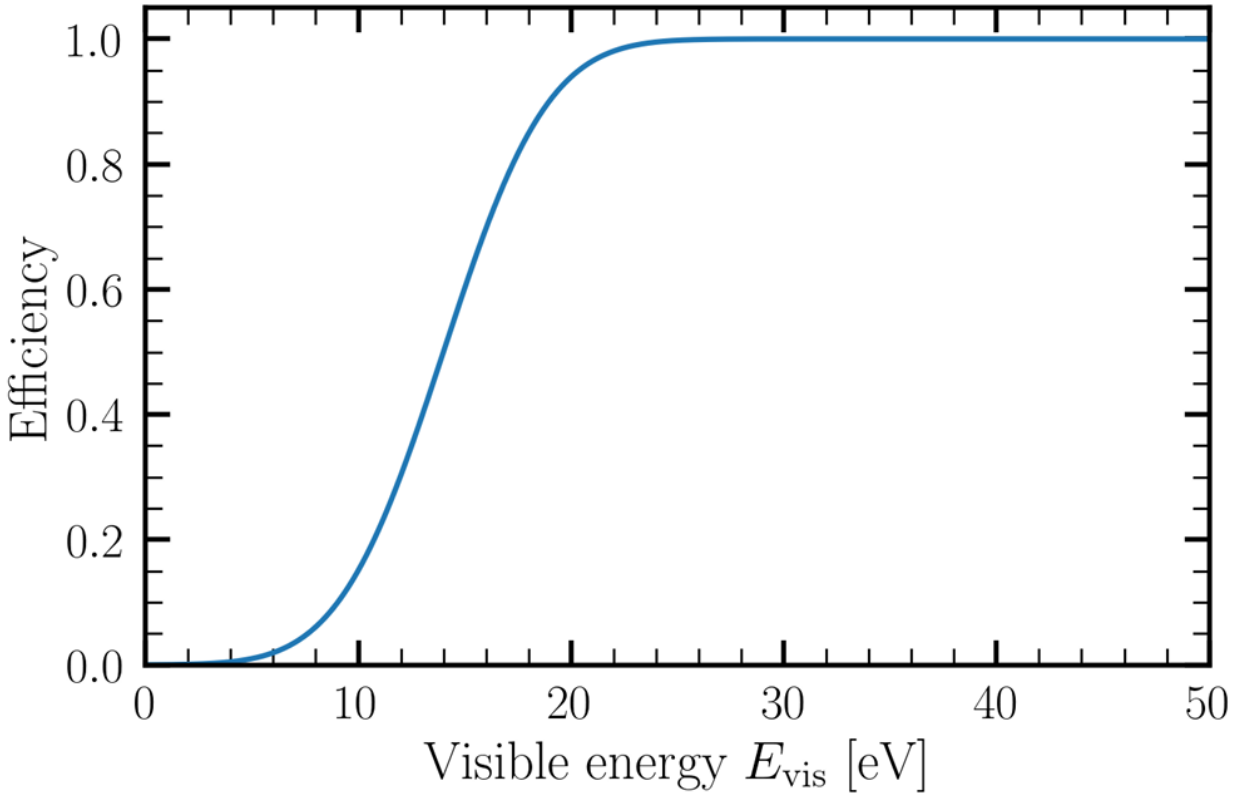
Efficiency
1.0
0.8
0.6
0.4
0.2
0.0
0
10
20
30
40
50
Visible energy E_{vis} [eV]

DarkSPHERE Parameters

Quantity	Symbol	Value
Detector and exposure		
Gas mixture	–	He:i-C_4H_{10} (90:10)
Pressure	p	5 bar
Target mass	M	27.3 kg
Exposure time	t_{exp}	300 days
Detector response model		
Energy threshold	E_{th}	0.014 keV
Threshold width	σ_{th}	3.876 eV
Fano factor	F	0.2
Polya parameter	θ	0.12
Analysis setup		
Background rate	B	0.01 dru
Energy window	E	$14\,\text{eV} \leq E \leq 1\,\text{keV}$
Confidence level	CL	90%
Number of bins	N_{bins}	25
Astrophysical input		
Local DM density	ρ_0	$0.3\,\text{GeV cm}^{-3}$
Circular speed	v_0	$238\,\text{km s}^{-1}$
Escape speed	v_{esc}	$544\,\text{km s}^{-1}$

Table 4.2: Parameters used for the DarkSPHERE experiment [6].

Limit Decomposition

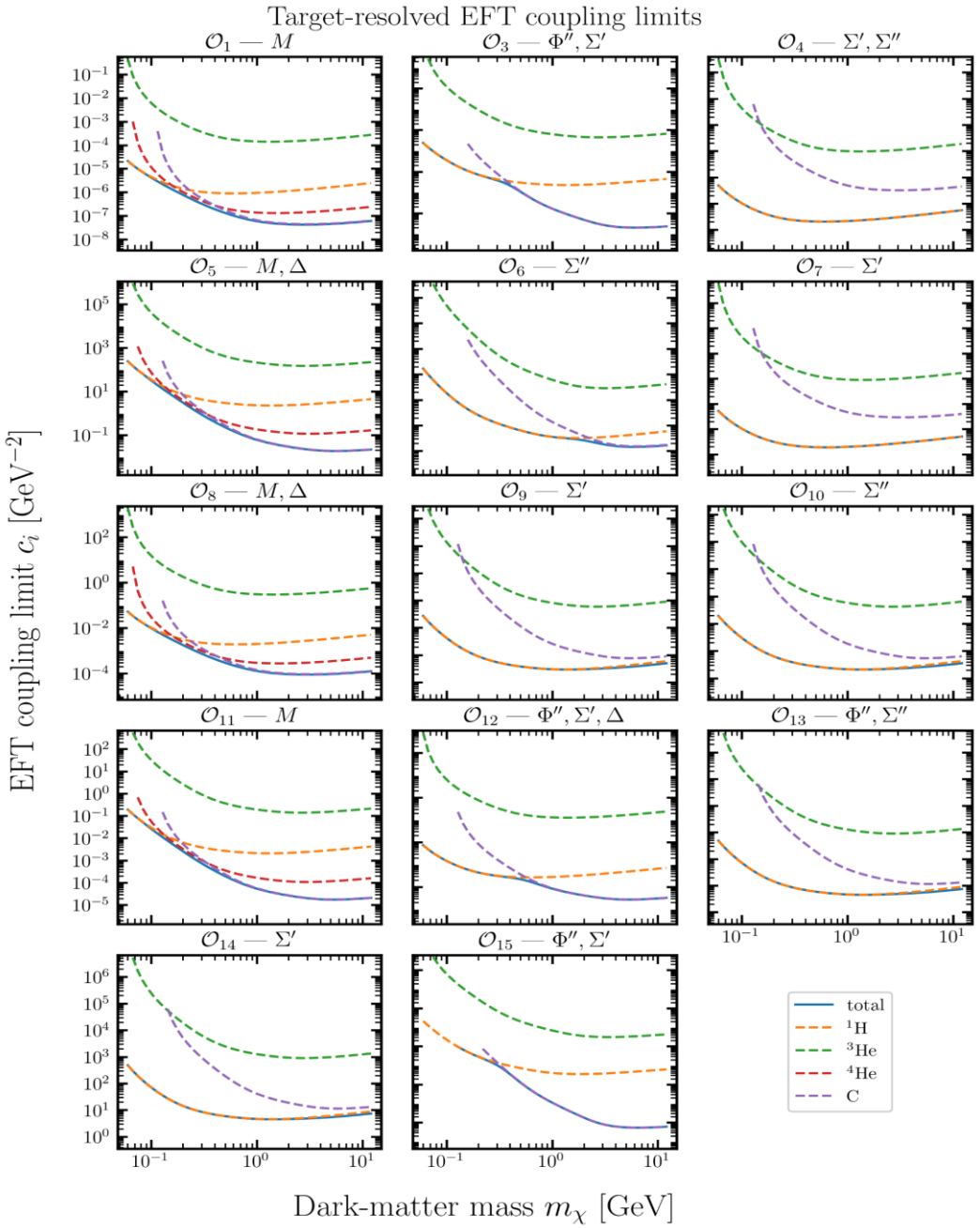

Grouped Operator Spectra

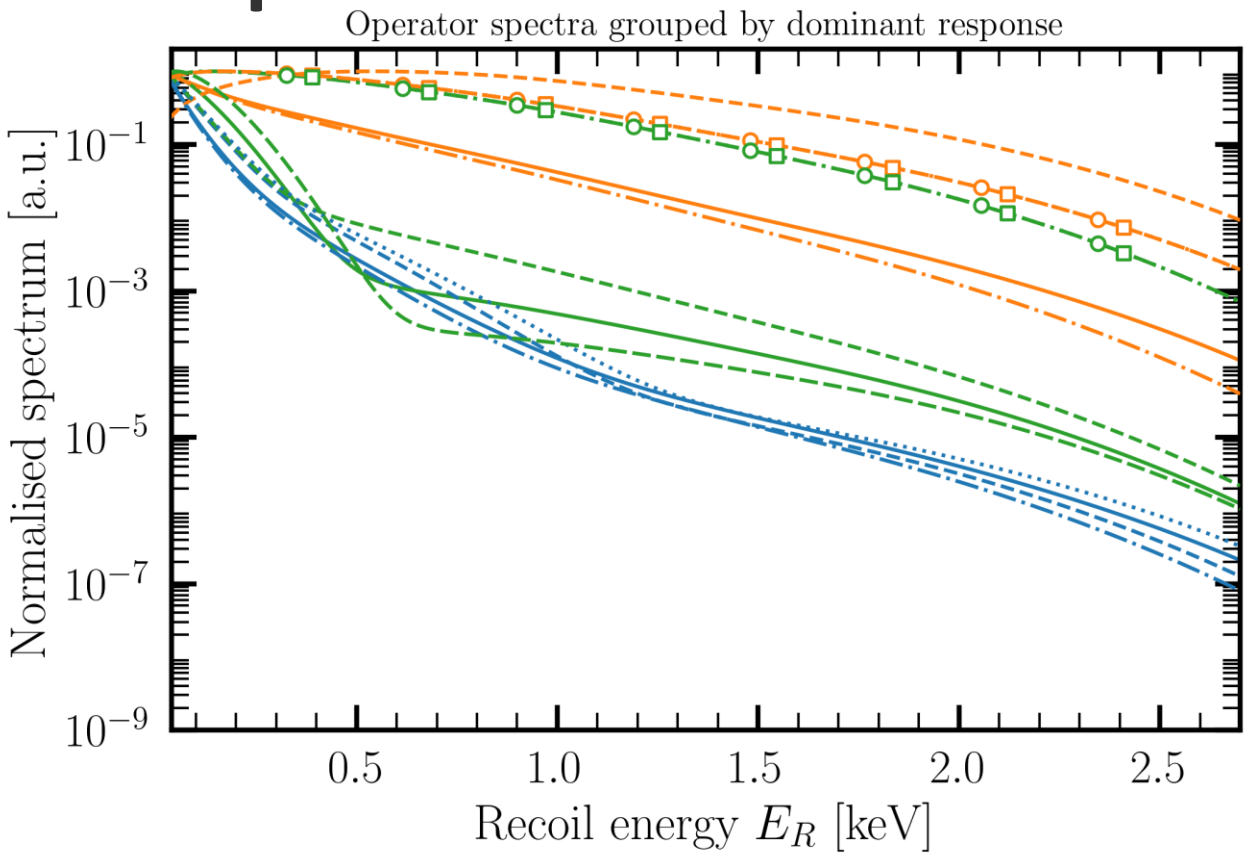

Coherent / charge-like	Spin-response dominated	Mixed / composite response
$\mathcal{O}_1$	$\mathcal{O}_4$	$\mathcal{O}_3$
$\mathcal{O}_5$	$\mathcal{O}_6$	$\mathcal{O}_{12}$
$\mathcal{O}_8$	$\mathcal{O}_7$	$\mathcal{O}_{13}$
$\mathcal{O}_{11}$	$\mathcal{O}_9$	$\mathcal{O}_{14}$
	$\mathcal{O}_{10}$	$\mathcal{O}_{15}$

Grouped Operator Spectra

Group	Operators
Coherent/charge-like	$\mathcal{O}_1, \mathcal{O}_5, \mathcal{O}_8, \mathcal{O}_{11}$
Spin-response dominated	$\mathcal{O}_4, \mathcal{O}_6, \mathcal{O}_7, \mathcal{O}_9, \mathcal{O}_{10}$
Mixed/composite response	$\mathcal{O}_3, \mathcal{O}_{12}, \mathcal{O}_{13}, \mathcal{O}_{14}, \mathcal{O}_{15}$

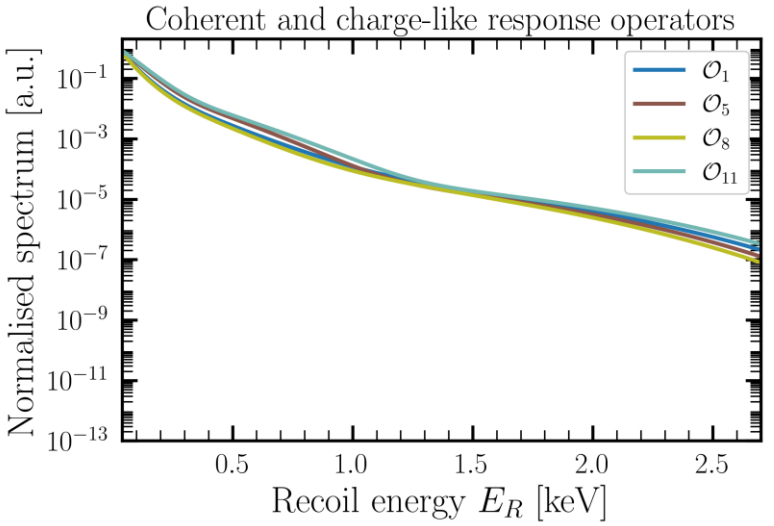

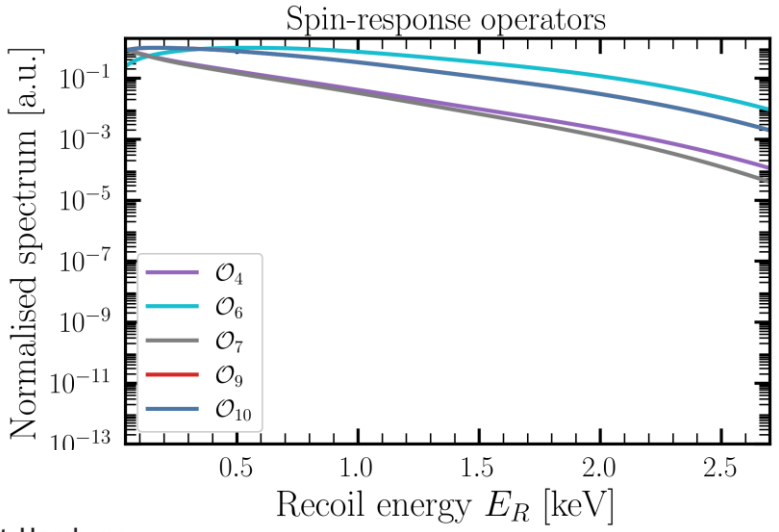

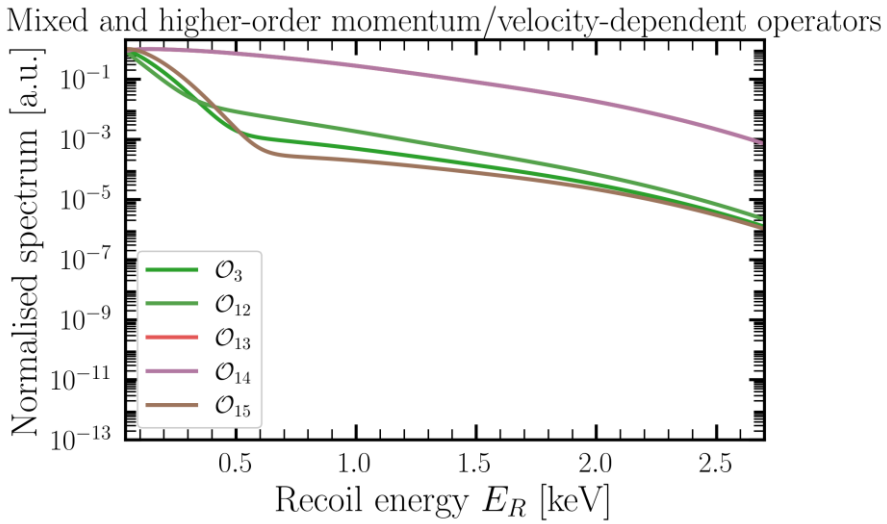

Grouped Operator Limits

- Grouping after similar responses

Group	Operators
Coherent/charge-like	$\mathcal{O}_1, \mathcal{O}_5, \mathcal{O}_8, \mathcal{O}_{11}$
Spin-response dominated	$\mathcal{O}_4, \mathcal{O}_6, \mathcal{O}_7, \mathcal{O}_9, \mathcal{O}_{10}$
Mixed/composite response	$\mathcal{O}_3, \mathcal{O}_{12}, \mathcal{O}_{13}, \mathcal{O}_{14}, \mathcal{O}_{15}$

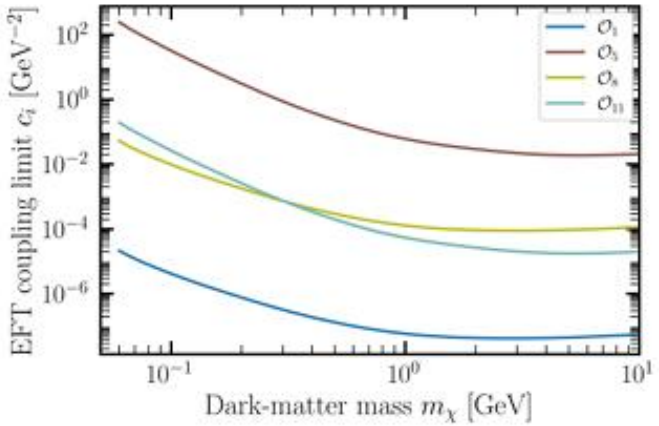

(a) Coherent/charge-like operators.

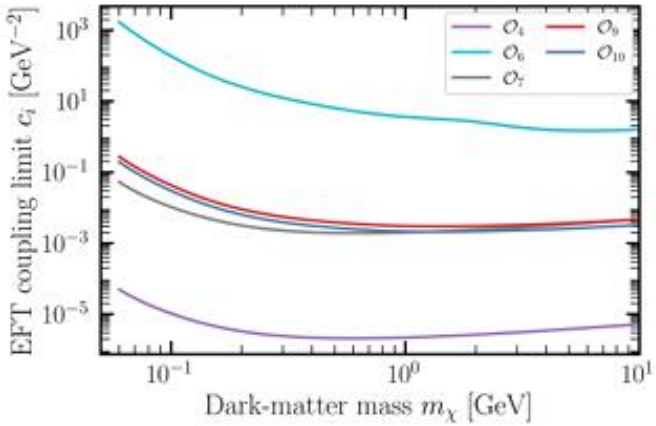

(b) Spin-response dominated operators.

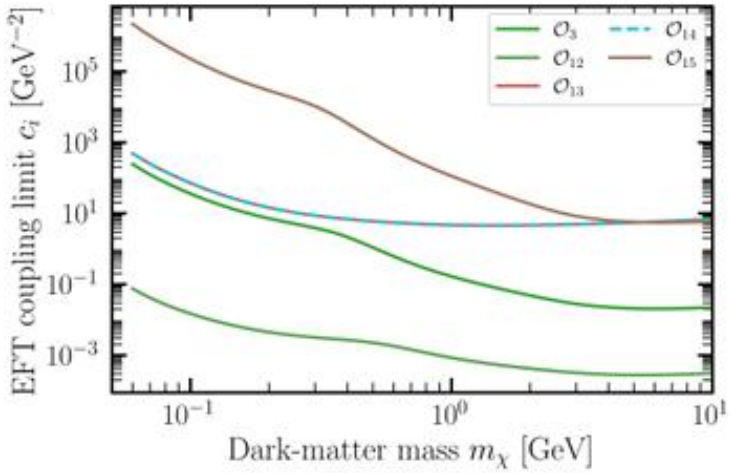

(c) Mixed/composite response operators.

Additional Groupings

Response/group	Operators	Interpretation/use
M		
M-type response	$\mathcal{O}_1, \mathcal{O}_{11}$	Operators with a pure or primarily coherent M-type nuclear response.
M, Δ		
$M + \Delta$ response	$\mathcal{O}_5, \mathcal{O}_8$	Operators receiving contributions from the coherent M response and the angular-momentum response Δ.
Σ', Σ''		
Spin-response operators	$\mathcal{O}_4, \mathcal{O}_6, \mathcal{O}_7, \mathcal{O}_9, \mathcal{O}_{10}, \mathcal{O}_{13}, \mathcal{O}_{14}$	Operators mainly associated with the transverse and longitudinal spin responses, Σ' and Σ''.
Φ''		
Spin–orbit/composite response	$\mathcal{O}_3, \mathcal{O}_{12}, \mathcal{O}_{15}$	Operators probing composite nuclear-response structures, in particular the spin–orbit response Φ''.
q-suppressed		
Momentum-suppressed operators	$\mathcal{O}_3, \mathcal{O}_5, \mathcal{O}_6, \mathcal{O}_{10}, \mathcal{O}_{11}, \mathcal{O}_{13}, \mathcal{O}_{14}, \mathcal{O}_{15}$	Operators with an explicit momentum-transfer dependence and therefore possible suppression at low recoil energies.

Table E.1: Grouping of the NREFT operators according to their nuclear responses and kinematic dependence.

Additional Groupings - Spectra

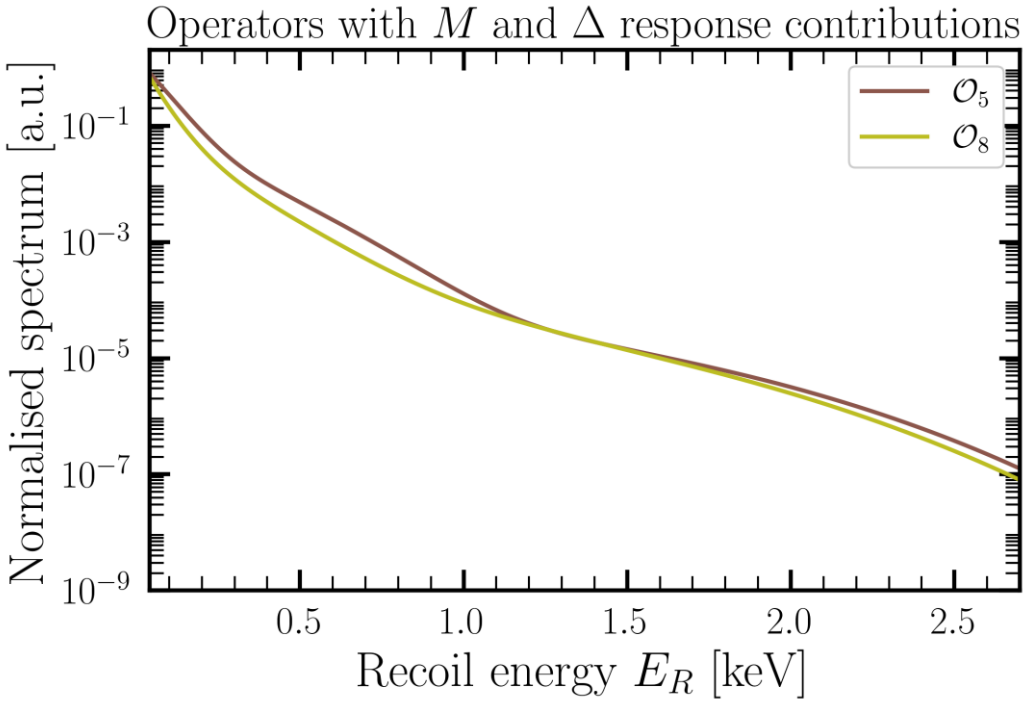

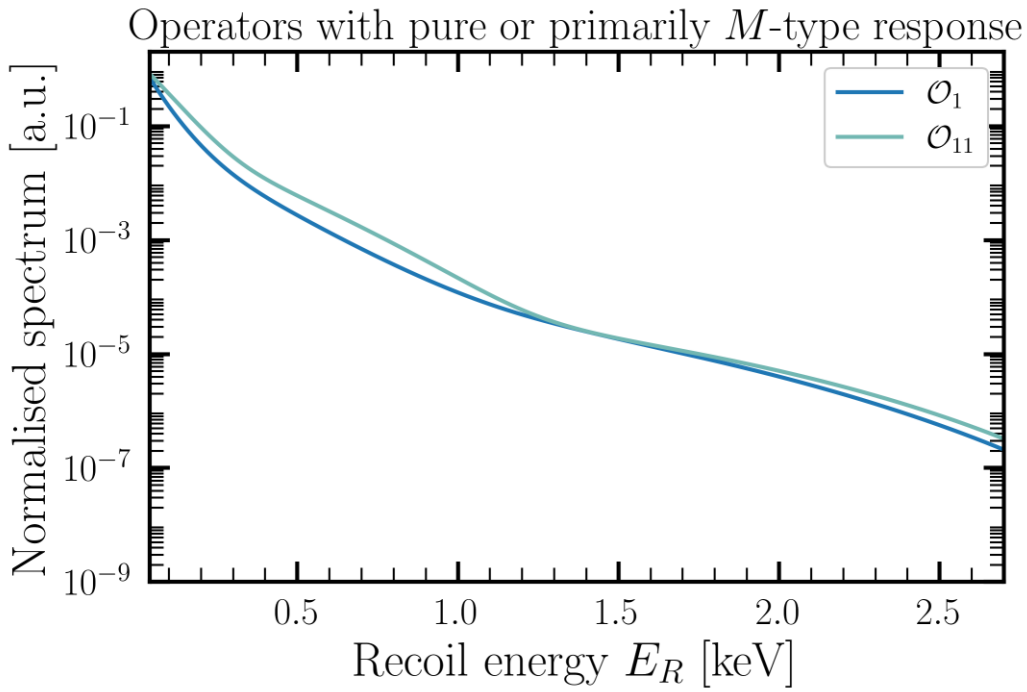

Additional Groupings - Spectra

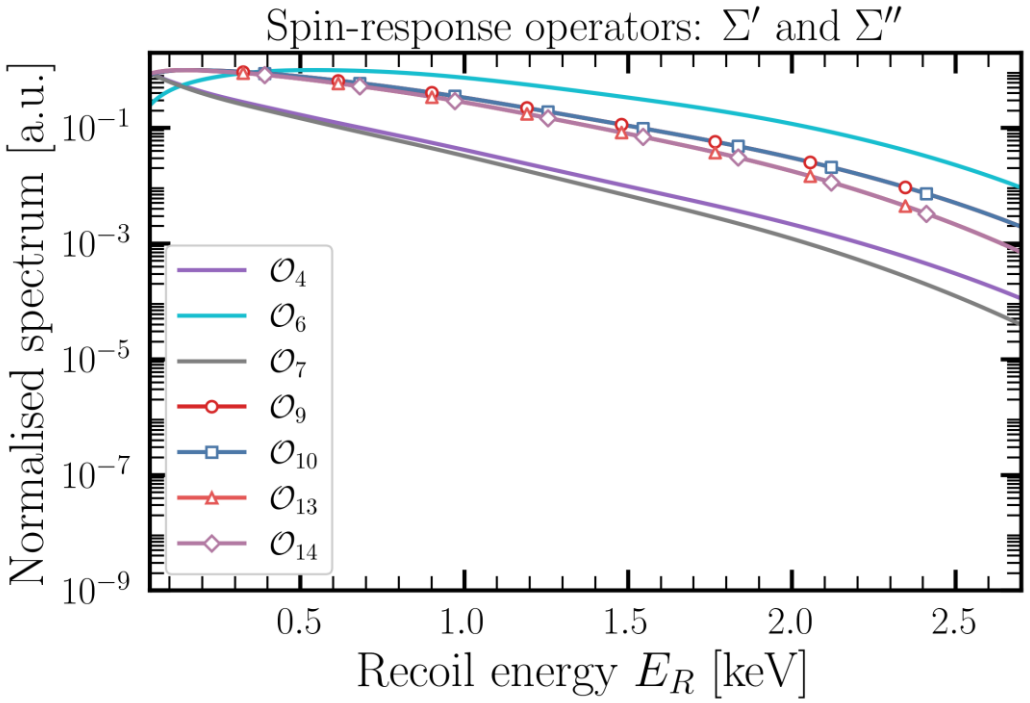

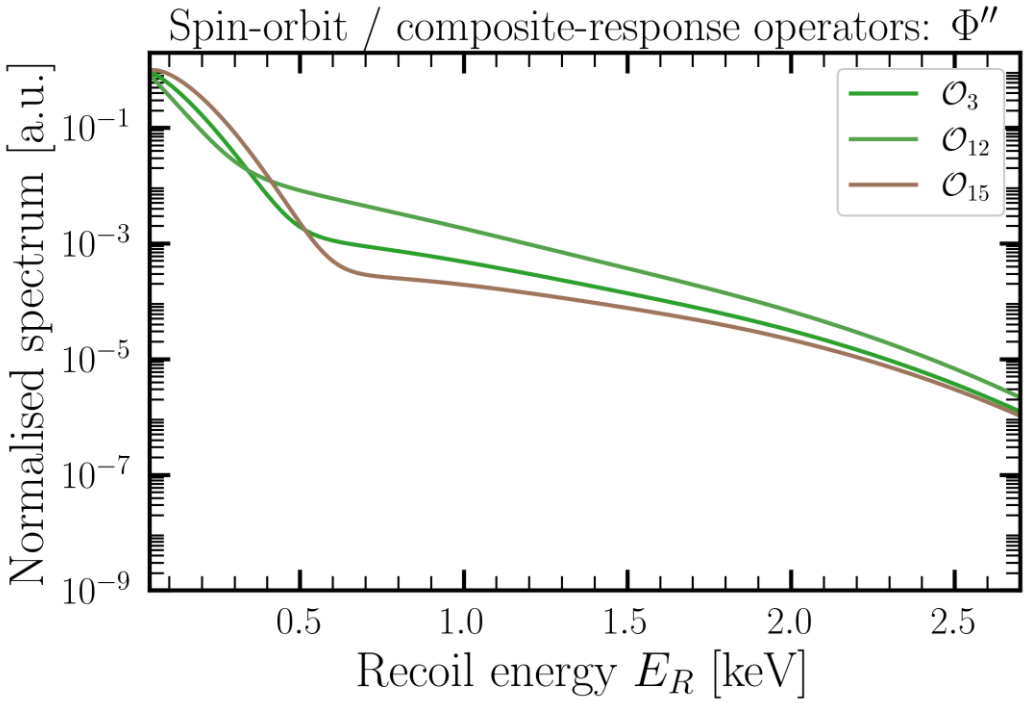

Additional Groupings - Spectra

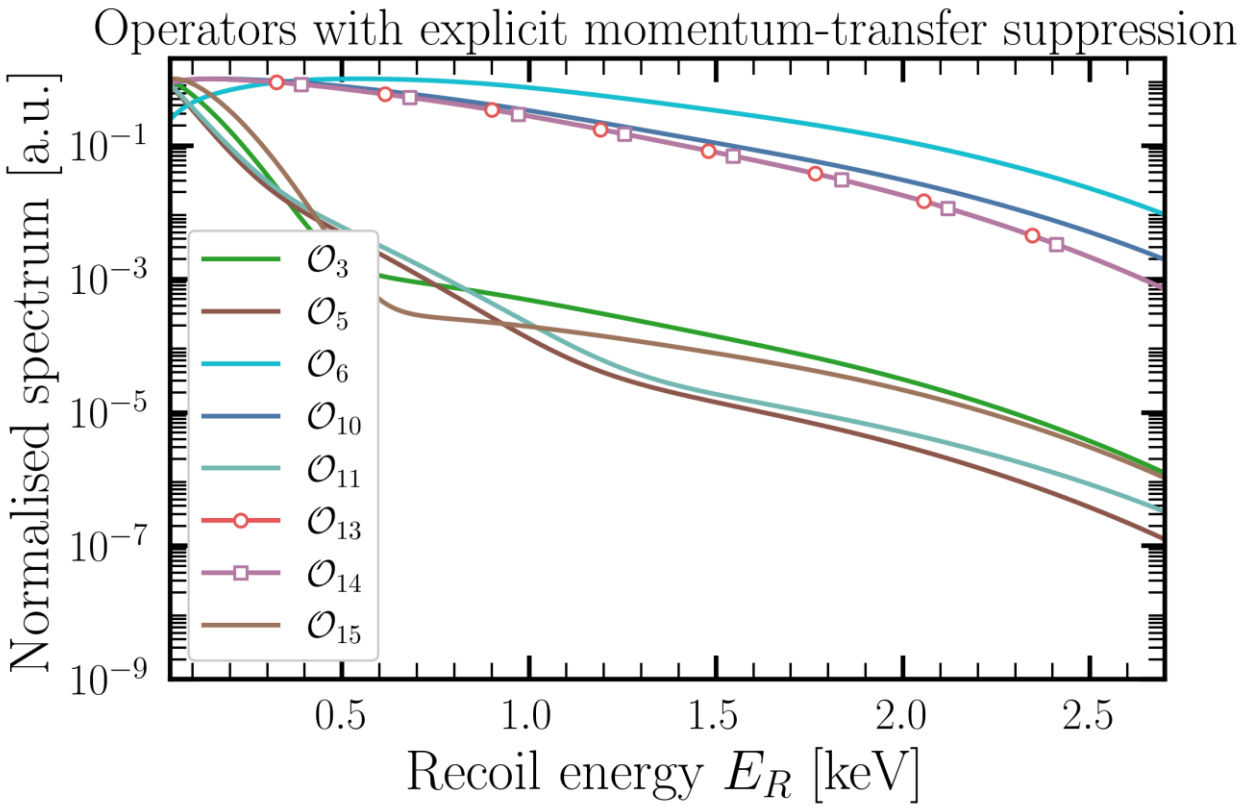

Additional Groupings - Limits

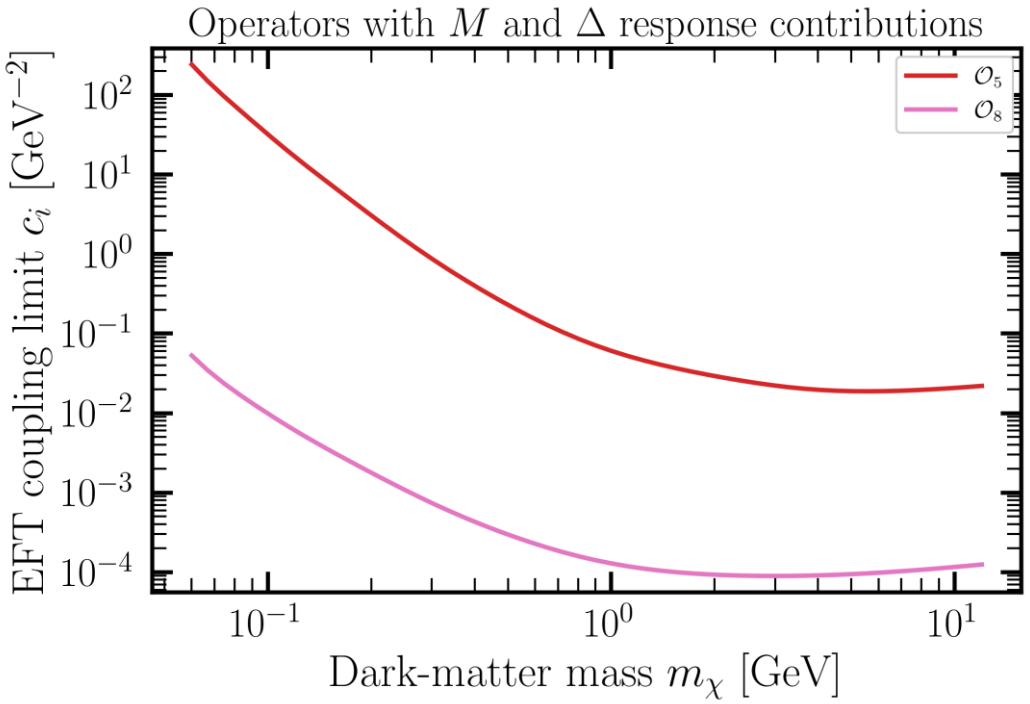

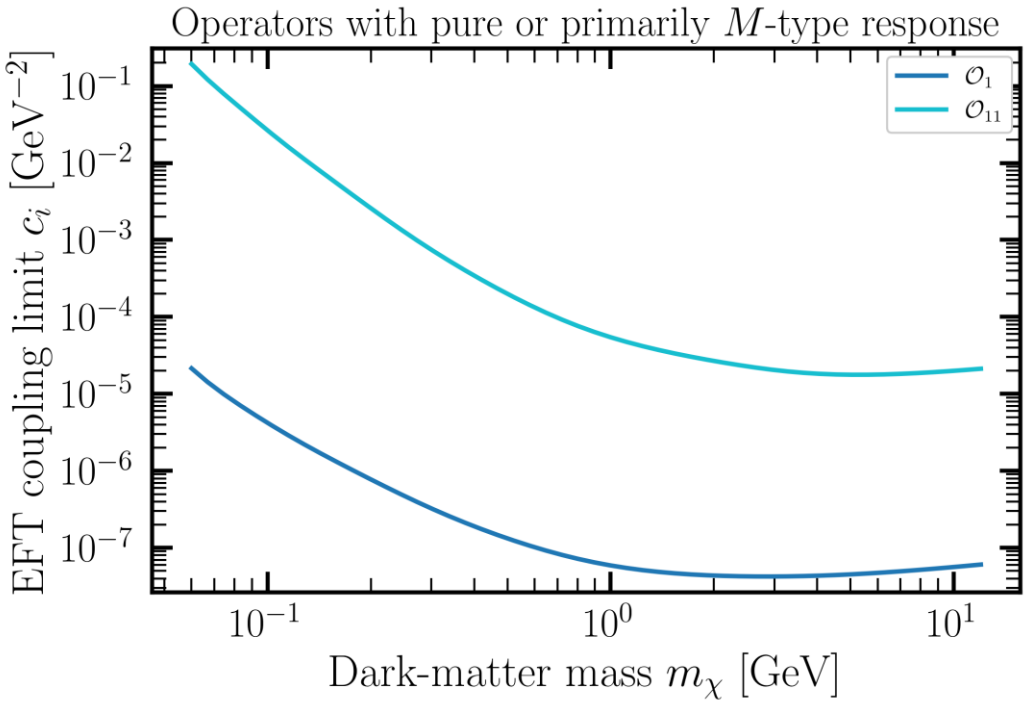

Additional Groupings - Limits

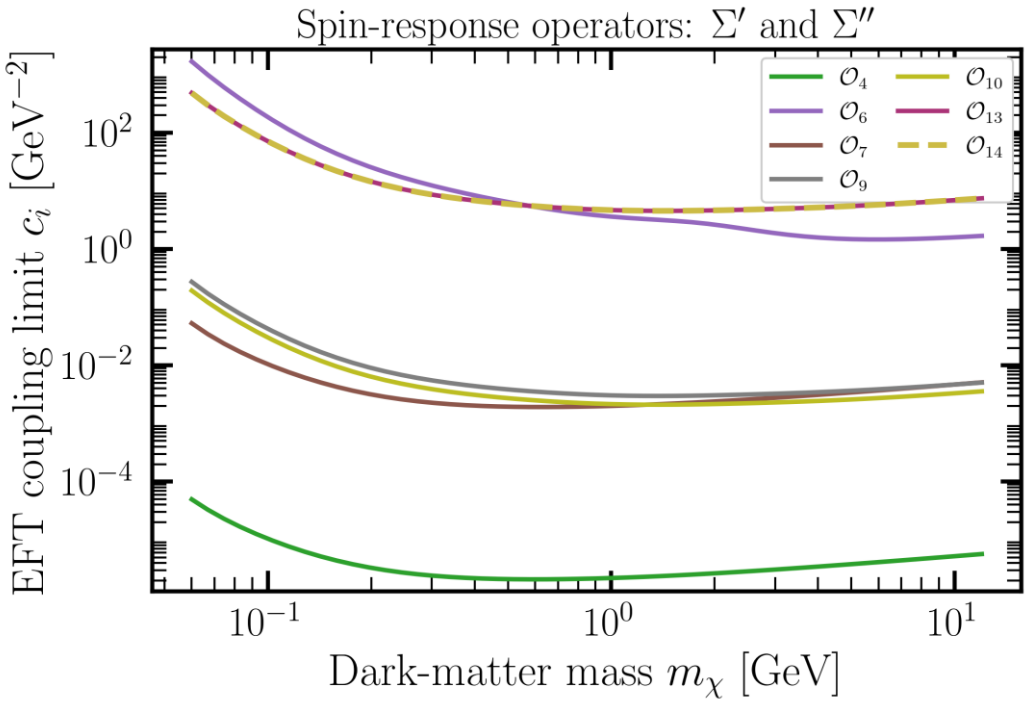

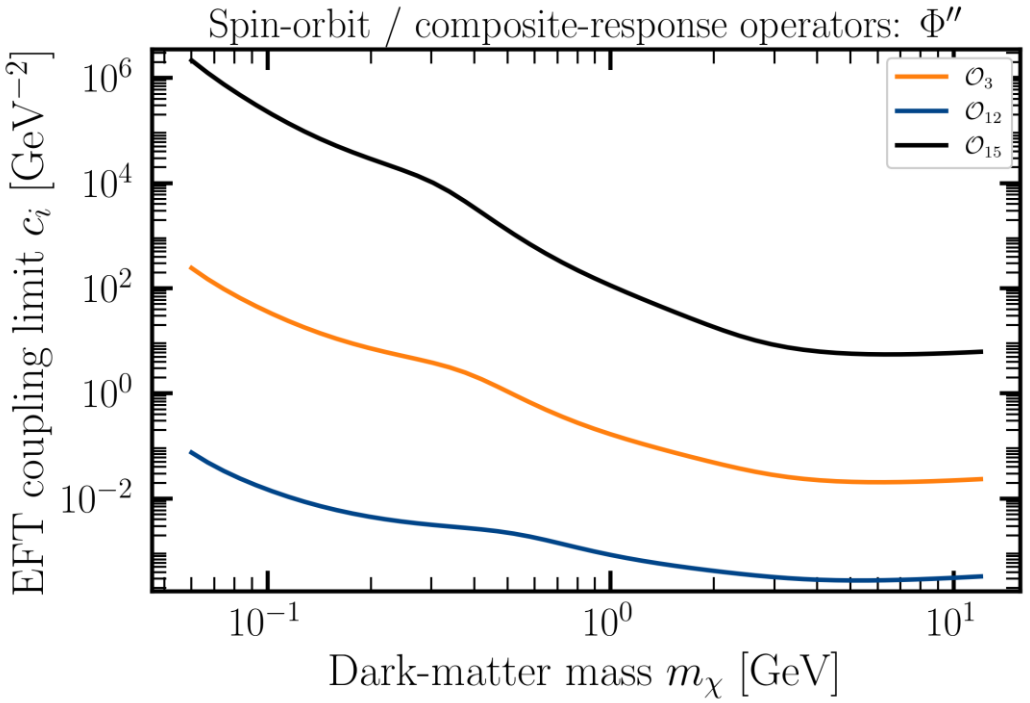

Additional Groupings - Limits

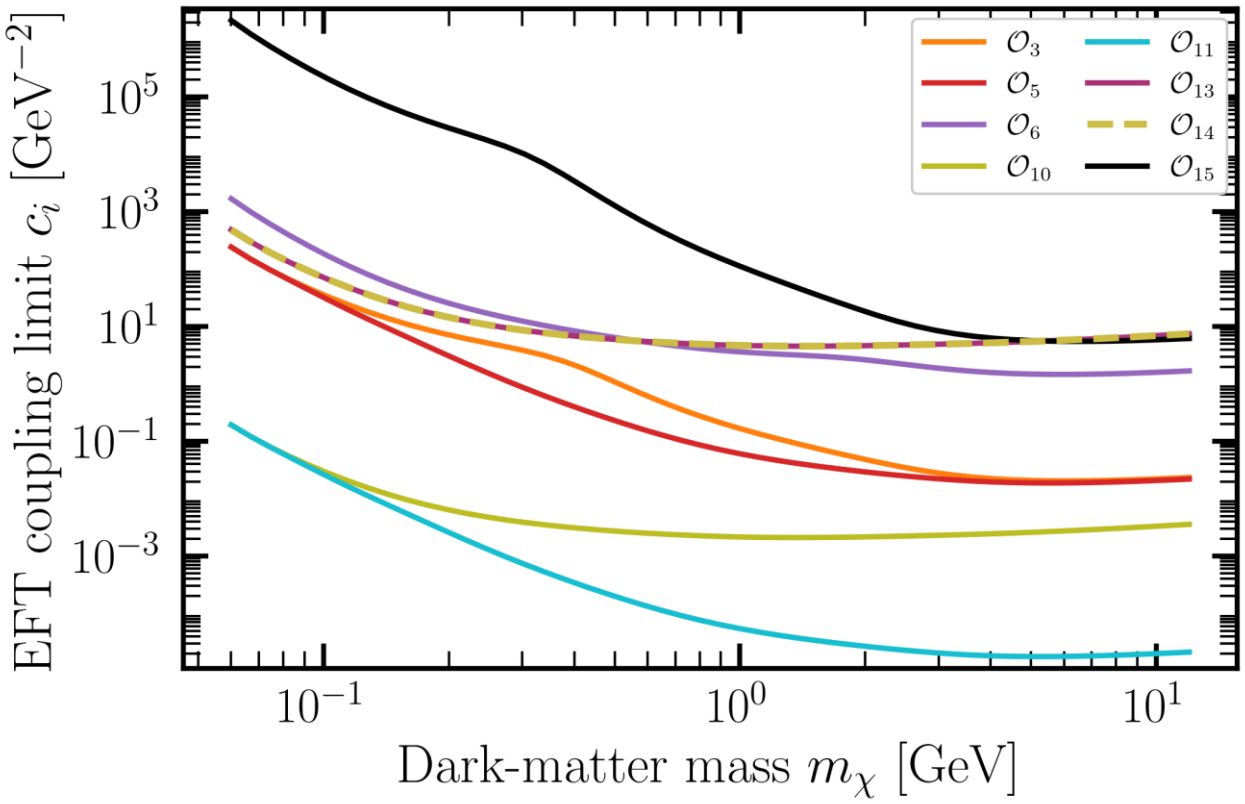

DarkSPHERE Sensitivity with DEAP exposure

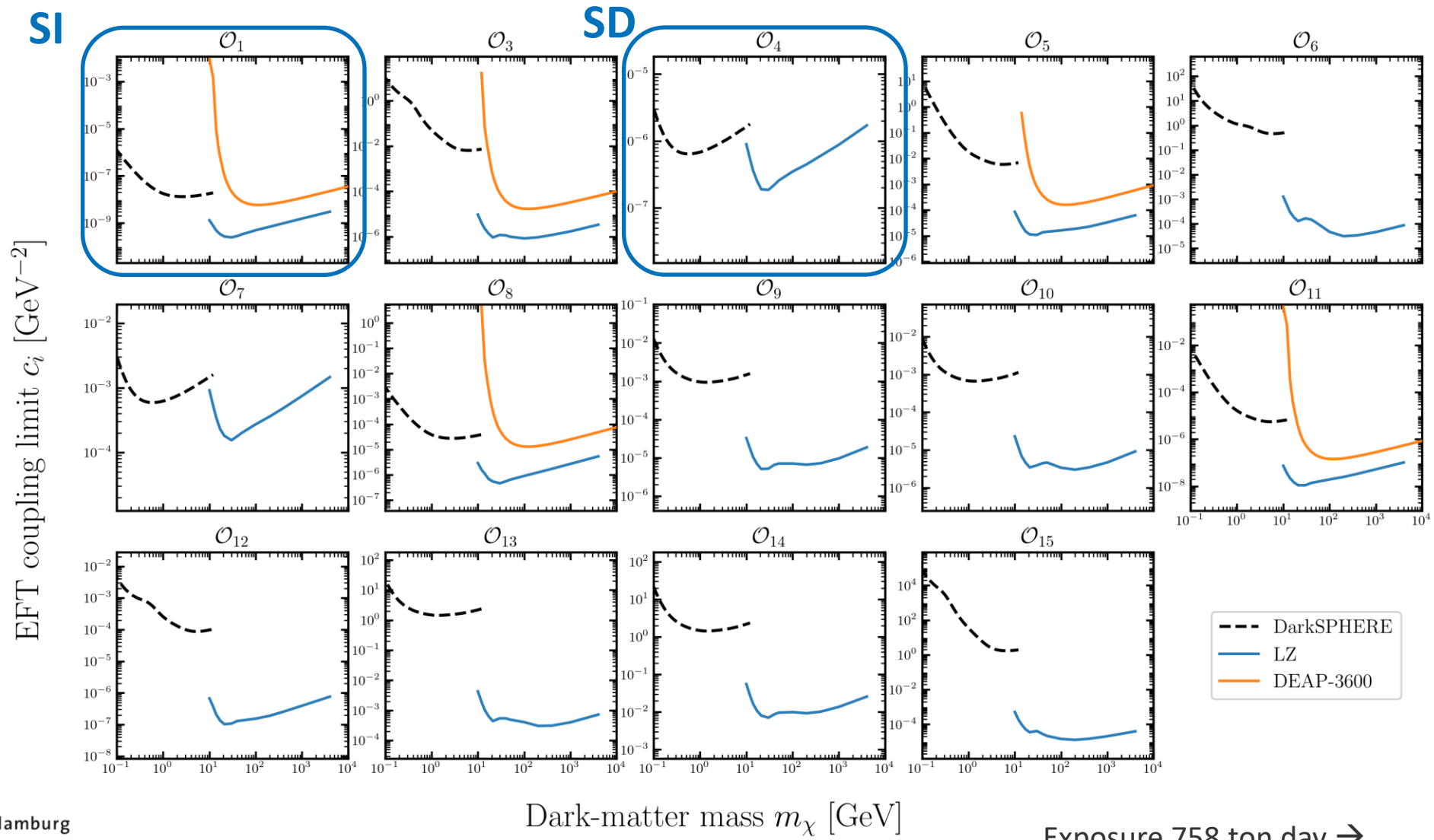

Exposure 758 ton day → 27765.5678 days/76 a

DarkSPHERE Sensitivity with LZ exposure

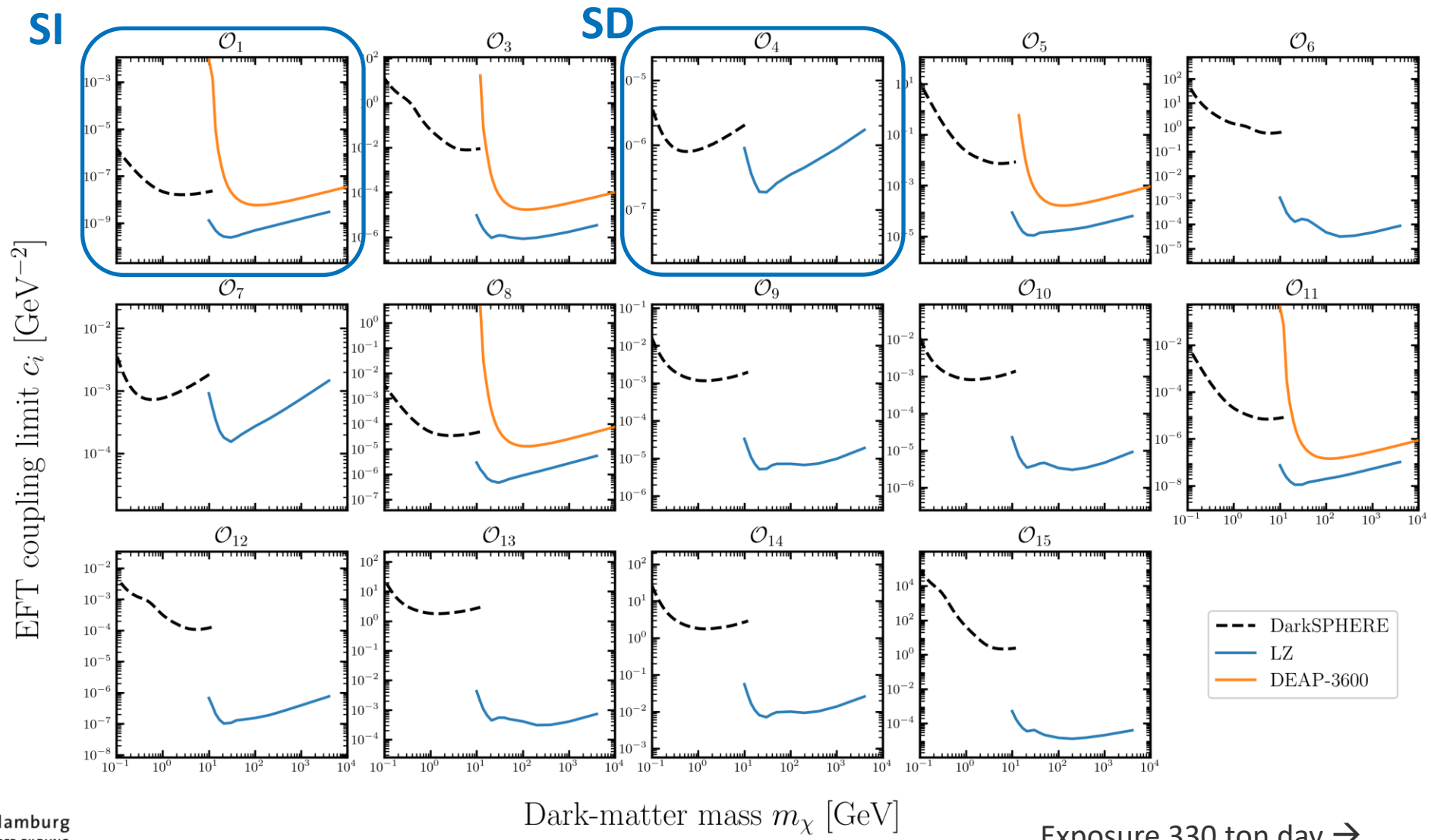

Exposure 330 ton day → 12087.9121 days/33.1 a

NN Inference of Dark Matter Masses from DarkSPHERE Spectra

- $\mathcal{O}_1$ (SI) interaction only
- Fixed halo + detector assumptions

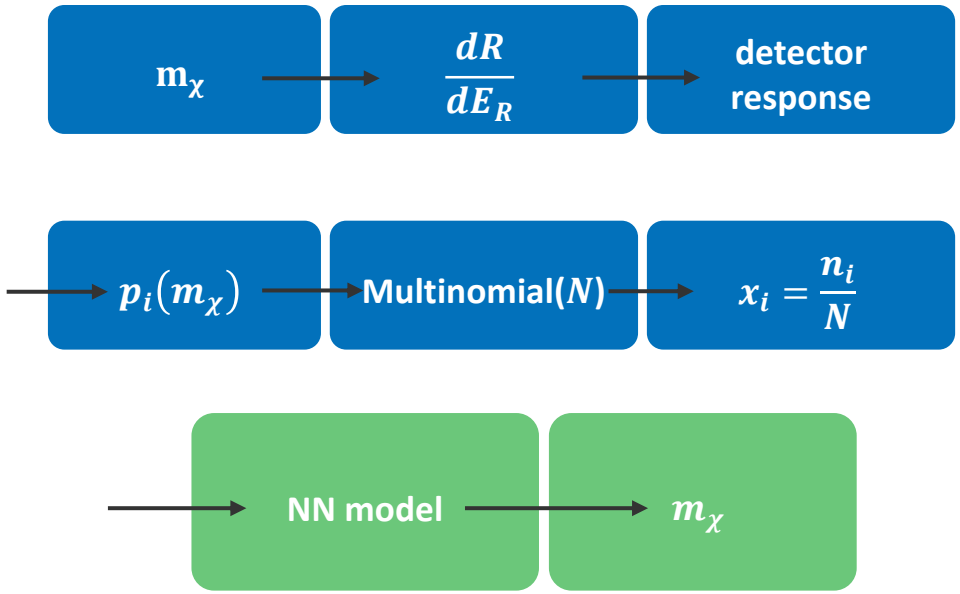

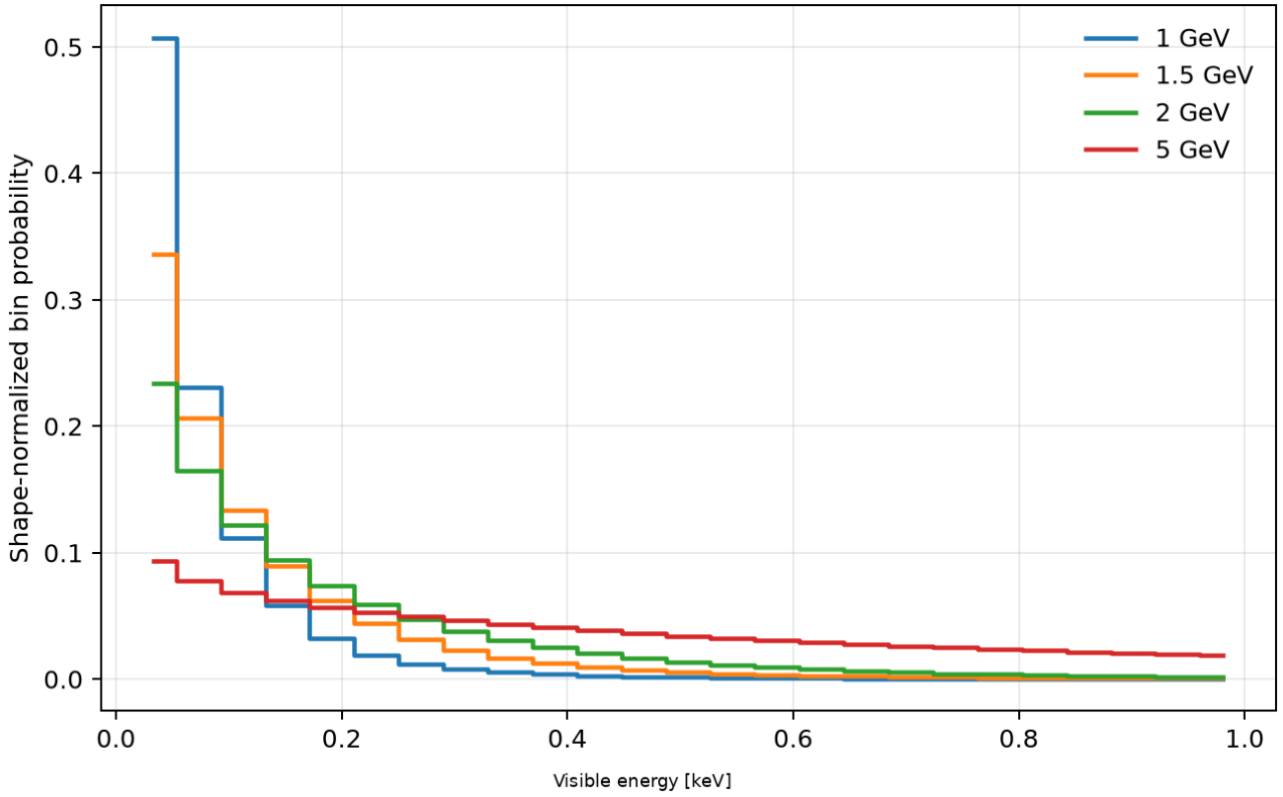

Combined Study Results

Classification

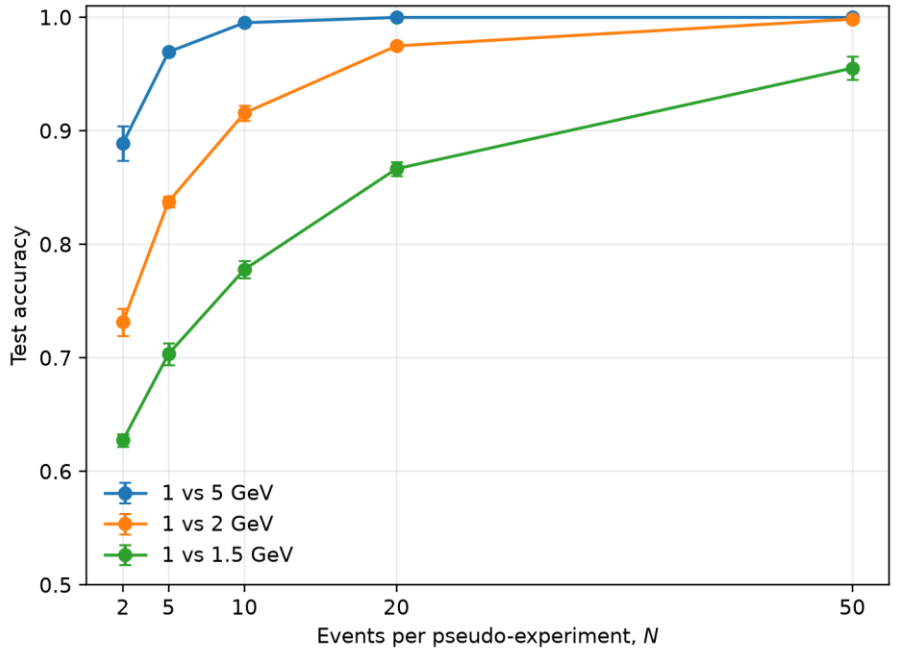

Regression

Model	log N	Multitask	MAE [GeV]
Shape-only regressor	No	No	0.47170
Conditioned regressor	Yes	No	0.46021 ± 0.00163
Shape-only multitask	No	Yes	0.47369
Conditioned multitask	Yes	Yes	0.46198 ± 0.00276

- $\Delta\mathrm{MAE}$ from $\log N \approx -0.0115$ GeV
- Best mixed-N tested model: conditioned single-output MLP

1. Mass inference possible, but limited by statistical fluctuations
2. Inclusion of log N modestly improves performance

Hyperparams

MLP baselines

Binary classifier

Linear: 25 → 2
Small MLP: 25 → 16 → 16 → 2
Large MLP: 25 → 64 → 64 → 32 → 2
Hidden activations: ReLU

Fixed-N regression

Small MLP regressor:
25 → 16 → 16 → 1
Output: standardized log10(m_chi/GeV)
No output activation

1D CNN baseline

Input reshape: (batch, 25) → (batch, 1, 25)

Conv1d(1, 8, kernel_size=3, padding=1)
ReLU
Conv1d(8, 16, kernel_size=3, padding=1)
ReLU
Flatten → Linear(400, 32) → ReLU → output

Padding detail: kernel size 3 with padding 1 preserves the 25-bin spectral length. No pooling was used.

Mixed-N multitask MLP

Encoder
25 or 26 → 32 → 32
ReLU after each hidden layer

Classification head
32 → 4 logits

Regression head
32 → 16 → 1
ReLU after 16-unit layer

Model type	Params
classifier + ln(N)	2,052
regressor + ln(N)	2,465
multitask + ln(N)	2,597

Training and losses

Setting	Binary	Fixed-N reg.	Mixed-N
Optimizer	Adam	Adam	Adam
Learning rate	1e−3	1e−3	1e−3
Batch size	256	256	256
Max epochs	100	150	150
Patience	10	15	15
Weight decay	0	0	0
Scheduler / clipping	none	none	none

Losses

Classification

Binary: CrossEntropyLoss
Mixed-N: weighted CrossEntropyLoss with four mass classes

Regression

MSELoss on standardized log10(m_chi/GeV)